



# Science and Technology of Additive Manufacturing Progress: Processes, Materials, and Applications

Vahid Monfared<sup>1</sup> · Seeram Ramakrishna<sup>2</sup> · Navid Nasajpour-Esfahani<sup>3</sup> · Davood Toghraie<sup>4</sup> · Maboud Hekmatifar<sup>4</sup> · Sadegh Rahmati<sup>5</sup>

Received: 16 April 2023 / Accepted: 5 May 2023 / Published online: 3 June 2023  
© The Author(s) under exclusive licence to The Korean Institute of Metals and Materials 2023

## Abstract

As a special review article, several significant and applied results in 3D printing and additive manufacturing (AM) science and technology are reviewed and studied. Which, the reviewed research works were published in 2020. Then, we would have another review article for 2021 and 2022. The main purpose is to collect new and applied research results as a useful package for researchers. Nowadays, AM is an extremely discussed topic and subject in scientific and industrial societies, as well as a new vision of the unknown modern world. Also, the future of AM materials is toward fundamental changes. Which, AM would be an ongoing new industrial revolution in the digital world. With parallel methods and similar technologies, considerable developments have been made in 4D in recent years. AM as a tool is related to the 4th industrial revolution. So, AM and 3D printing are moving towards the fifth industrial revolution. In addition, a study on AM is vital for generating the next developments, which are beneficial for human beings and life. Thus, this article presents the brief, updated, and applied methods and results published in 2020.

**Keywords** 3D printing · Additive manufacturing · Medical sciences · Tissue engineering

## 1 Introduction

In recent years, Additive Manufacturing (AM) technology has developed extensively and has proved huge potential in industrial, biomedical, and bioengineering applications. For example, AM's technological development enables a circular economy to be created by dispersing recycling and manufacturing. Circular economy “circularity” is a mechanism and

system purposed to remove waste (Fig. 1). The concept of Dispersed Recycling by Additive Manufacturing (DRAM) involves using reprocessed materials in the AM procedure chain through mechanical recovery.

Robots, quick networks of data, and interconnected devices enable the fourth industrial revolution to make factories more creative and carry out tasks better handled by machines. The fourth industrial revolution (such as AM or 3D printing technology as a tool) starts to go towards the fifth industrial revolution while you start to let customers customize what they want. The fifth industrial revolution takes the idea of personalization to the next level. Furthermore, several possibilities for the future of AM technologies may be in the medical sciences and tissue engineering such as “manufacturing the device for controlling the heart performance”, “manufacturing the virus fast detection kits”, and “producing the quasi-real human organs”. For instance, AM (the fourth industrial revolution) can be very useful in challenges posed by COVID-19 (AM/3D-printing→5th industrial revolution). In addition, AM is going to create smart materials with 3D printing technologies shortly.

✉ Vahid Monfared  
vahid\_monfared\_57@yahoo.com

✉ Davood Toghraie  
Toghraee@iaukhsh.ac.ir

<sup>1</sup> Department of Mechanical Engineering, Zanjan Branch, Islamic Azad University, Zanjan, Iran

<sup>2</sup> Department of Mechanical Engineering, National University of Singapore, Singapore 117574, Singapore

<sup>3</sup> School of Material Science and Engineering, Georgia Institute of Technology, Atlanta 30332, USA

<sup>4</sup> Department of Mechanical Engineering, Khomeinishahr Branch, Islamic Azad University, Khomeinishahr, Iran

<sup>5</sup> Department of Medical Science and Technology, IAU University, Central Branch, Tehran, Iran

It should be mentioned that 3D printing has the potential of transforming the present manufacturing approaches soon [1–7]. Fatigue is a predominant failure mode and fatigue modelling was done in some Refs. [8–10]. Inherently defective metal AM parts require optimization of cyclic mechanical approaches since fatigue is a predominant failure mode.

Furthermore, this review article examines the latest explanations as a suitable investigation of the research works on the results in AM in addition to the circular/linear economy aspects and the following top ten advantages of AM. The top ten advantages of AM are as the following,

- The cost of entry will become more reasonably priced
- It decreases waste production, and it saves on energy costs
- The prototyping costs would be much less
- Small production runs often show quicker and less expensive
- You don't require as much on-hand inventory
- It's easier to reconstruct and optimize old parts (it is simple to change or modify versions of a product)
- You may get better part credit and validity
- You can strengthen an assembly into a single part (DFAM)
- It independently supports novel AI-Driven design methods (and training programs are becoming readily accessible at All levels)
- It solely supports lattice structures

So, the major aim of this research article is to collect the results of the novel and applied for research works as a beneficial package for researchers. At the end of the conclusion, different diagrams, infographics, and obtained results (as a conclusion of this article) are presented. The research article [11] explains the combined artificial intelligence (AI) and plasma emission spectroscopy (PES) to recognize the porosity of AM pieces. It also demonstrates the enormous potential and challenges of PES for AM laser-quality monitoring. Laser quality can prove the enrichment of AM techniques. Therefore, it is a very important factor. Figure 2 shows the accuracy of recognition in terms of print layers. Figure 2 shows RF testing outcomes and results for dense and porosity recognition. Following Fig. 2, as the number of print layers increases, the detection accuracy reduces in all samples. This decrease is due to the thickness of the deposition [11].

## 2 Some Important Points

Here, it is required to indicate and illustrate some highlighted and significant related topics and features like ASTM standards along with answering some related questions about additive manufacturing AM briefly.

### 2.1 ISO/ASTM52900

In general, ISO/ASTM 52,900 defines the terms used in additive manufacturing (AM) technology, which applies the additive shaping principle to build physical 3D geometries by successively adding material. There are specific fields of application for each of the terms.

By promoting knowledge of additive manufacturing AM, encouraging research, and encouraging technology adoption, ASTM's standards contribute to the advancement of industry knowledge. Standards also define terminology, measure productivity, and describe procedures for calibrating additive manufacturing machines, which contribute to a better end product. There are also descriptions of applications, designs, materials, and processes, as well as test methods included in this standard. It is important to note and attend to some withdrawals, like F2792-12a standard terminology for additive manufacturing AM technologies (withdrawn 2015).

For another example, it is presented the scope for “ASTM ISO/ASTM52921-13(2019) Standard Terminology for Additive Manufacturing-Coordinate Systems and Test Methodologies” as the following. To standardize the terminology used by AM users, producers, researchers, educators, the press/media, and others when reporting results from testing parts made on AM systems, this terminology includes terms, definitions of terms, descriptions of terms, nomenclature, and acronyms related to coordinate systems and testing methodologies. The terms comprised cover definitions for machines/systems and their coordinate systems plus the location and orientation of parts. Aiming to comply with ISO 841 where possible and clarifying how those principles can be applied to additive manufacturing, it will, where possible, follow those guidelines. Additionally, there are two notes for that. In the first part, it states that the standard needs to be evaluated to determine whether it applies to cladding. And the second one is “Non-cartesian systems are not covered by this standard”. For more information, please check the ASTM website ([www.astm.org](http://www.astm.org)).

### 2.2 Some Comments and “Answers Questions” About AM

Answers regarding AM are ways to use the researchers' experiences [12, 13]. There are presently two large gaps: one lacks computational capabilities, and another is scalability. The first one can precisely explain and predict properties. Genetic algorithms (GA) or machine learning techniques (MLT) can predict and detect data defects. Therefore, predicting defects can help a lot in the development of manufacturing techniques [12]. As manufacturing society develops computational techniques and scalability, a focus is being placed on scalability. Currently, MLT and GA are buzzing

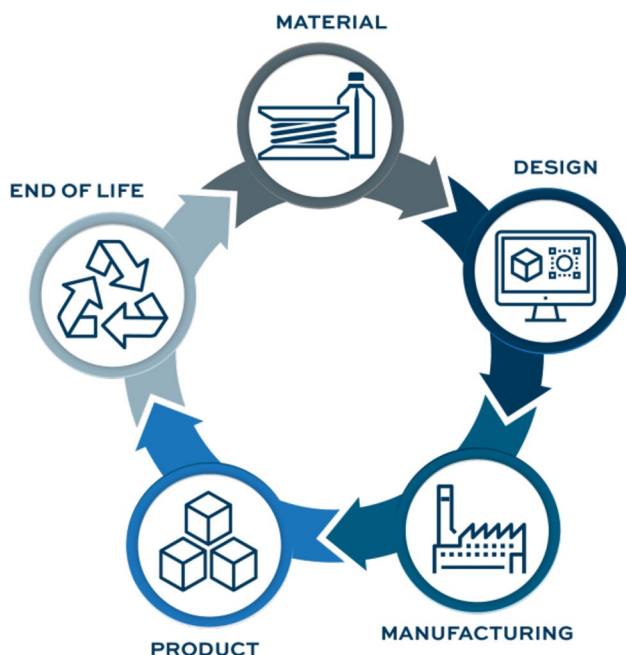


**Fig. 1** The circular economy unites the entire supply chain

topics in AM, which were previously developed in other contexts [2]. Different disciplines can use AM to create a common language [13]. Thus, it is a pricey method. Hence, applying this technique in any field is of substantial value [14].

In addition, AM proposes advantages in the field of biomedical engineering like tissue engineering or drug delivery. This technology employs digital design for high-accuracy manufacturing [5]. AM can offer solutions for human-scale vascular construction. In addition to the pathway to regulatory approval challenge, another challenge is the variety of biomaterials appropriate for AM procedures. It is extensively used in the digital fabrication and design of biomaterial models and drug delivery systems. [15].

Changing the connectivity of a motif design is analogous to changing the shape of macroscale structures. No energy is required for massive changes in shape in the molecular network. A connection of this type would facilitate the development of new chemical and material functions and construct new activation and response mechanisms [16]. AM accepts the use and printing of three-dimensional designs of metal parts, single crystals in harsh environments, and site-specific chemical compounds. The future of metal printing will be enabled by combining the science of metallurgy with the rapid development of new digital tools, such as machine learning and mechanical models. From product design to process monitoring and planning, these tools may assist the progress of microstructure and attributes, accelerate part qualification and automate part inspection [17].

### 3 Use of 3D-Printing and AM in Bio-Applications, Biomedical and Tissue Engineering

Here the applied and considerable research work results are presented [18–27]. It may be possible to change the bioinspired design process in future research, a repetitive design process for creating new bioinspired architectures via additive manufacturing [18]. Shortly, similar techniques and methodology may be utilized to guide additional progress of bighorn sheep velar bone bioinspired energy-storing material architectures for other applications (Figs. 3, 4). Which, the reiterative design process is shown in Fig. 3. Figure 4 Displays the relationship between stiffness and impact force as the following.

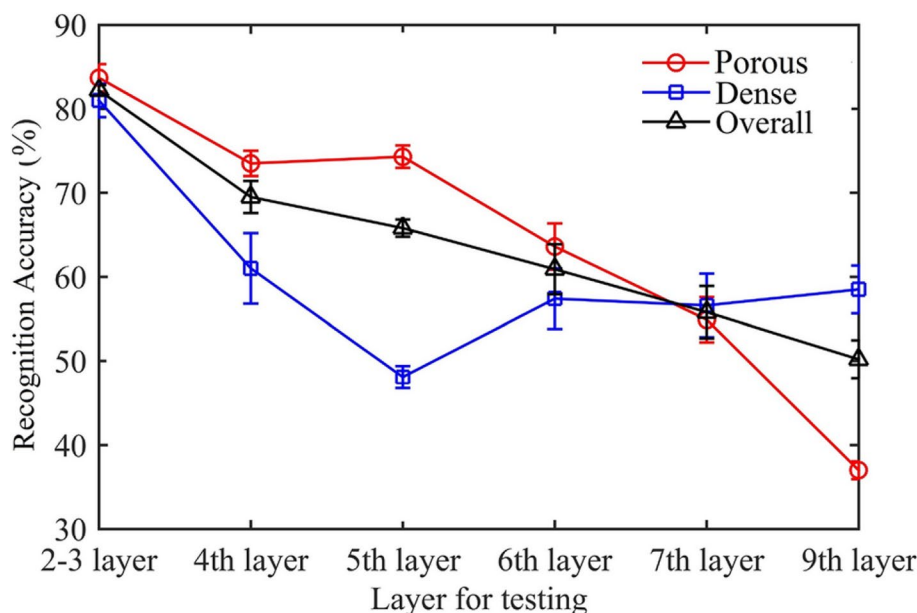
The revealed advances show that O3DP applications can be expanded by opening the way for multi-scale manufacturing out of a single bio-based material non-depending on the employed gadget [19]. The use of two-photon AM to fold two-dimensional channel layouts into compact free-form three-dimensional fluidic circuits with nanometer precision has been presented [20].

AM is used in various applications, such as splitters that multiply ventilator capacity, ventilators, guards, 3D bioprinting, swabs for testing, lung models, and oxygen valves. As a result, the Coronavirus has been weakened. Generally, researchers are advancing this algorithm by considering the regions that used AM during the coronavirus, conducting an AM survey, and analyzing it [21]. Figure 5 displays how AM may be useful in response to the coronavirus. Coronavirus has brought much instability and turbulence among manufacturing organizations. This algorithm can also help additive manufacturers during an epidemic [21].

AM is widely used in other medical fields such as in-vitro technology, the pharmaceutical industry, drug delivery, 4D printing, etc. AM is used in the pharmaceutical industry by various methods, SE-AM and SLA. These methods are used for diagnostic processes in the medical field. Also, melt-electrospinning writing (MEW), fused deposition modeling (FDM), and selective laser sintering (SLS) methods are used for making and external prostheses. And SE-AM is mostly used in polymer structures. As well as the development of advanced materials engineering tools, digital control, and permanent automation of the production method, will have a significant impact on the biomedical industry [22].

Organic polymers play a vital role in the medical community in general. To test these polymers, scaffolds for tissue engineering are infused with cells or growth factors [23, 24]. To determine their clinical role in bone scaffolding and medical field performance, these polymers should be investigated using AM methods. It is possible to solve the problem of high physical and biochemical gradients in applications

**Fig. 2** The change in recognition accuracy in terms of print layers [1]



such as tissue engineering and artificial organ development by evaluating pH within the cellular environment. With this method, more advanced and smart biological scaffolds can be used. The important number of studies about this topic underscores the importance of AM in enabling the future of health care. It is rational to suppose that the healthcare sector can expect new paradigms in AM technologies [25]. Figure 6 schematically presents the 3D bioprinting steps.

A new AM-assisted IC route has been described for developing indigenously  $HA/TiO_2$  coated biodegradable AZ31B alloy [26]. P-H-C composites are widely used for bone repair materials. The distribution of the P-H-C matrix can be shown by scanning electron microscope (SEM) analysis. Finally, for the thermal stability of this composite, differential scanning calorimeter (DSC) analysis is used [27].

#### 4 Other Important Applications of AM and 3D-Printing

Superalloys with approximately equal Ni, Co, Al, Cr, Ta, and W have high-strength prints. These superalloys are defect-resistant and possess over 1.1 GPa in as-printed and post-processed forms. The principles of these alloy designs can be explained by examining the structure of SLM and EBM CoNi base materials. After cross-sectioning the samples in half along the build direction, electron backscatter diffraction (EBSD) maps of post-mortem specimens were gathered together [28]. Also, for obtaining the apparent distribution coefficient, the Scheil equation is used (Eq. 1),

$$C_s = kC_0(1 - f_s)^{k-1} \quad (1)$$

At which  $C_s$  is the concentration of the solid, and  $k$  represents the distribution coefficient ( $k = C_s/C_l C_0$ ), and  $f_s$  represent the fraction solidified, [28]. It is possible to synthesize metal composites using IHT sequences controlled digitally. Layer-wise fabrication is the method used to make this method. In other words, the martensitic steel nanostructure is used. The opportunity to mechanical attributes and locally tailor microstructures provides new possibilities for manufacturing. For instance, the outer skin is hardened with precipitation, and soft and tough tools are produced inside. [29].

In Fig. 7, the Gibbs free energies of  $Fe_{19}Ni_{1-x}Ti_x$  alloy at different Ti are represented (at room temperature). This structure consists of a single-phase bcc and FCC, and the Ni content of 19 wt% is considered fixed [29].

Figure 8 Represent the diagram phase of the  $Fe_{19}Ni_{1-x}Ti_x$  (wt%) alloy [29]. To thermally manage the potential of the protocols, printed silica aerogel objects are used [30]. The 3D printing procedure opens novel uses for silica aerogels. Consumer electronics and thermal insulation devices will be made miniaturized by AM. The VOC degradation system and Light-driven gas pump devices are represented in Fig. 9 [30]

Biological and electronic inks have been analyzed for in situ 3D printing, open-loop, and predictive control [31]. The remelting of SLM-processed layers is a new metallurgy engineering technique. This method involves melting powder with a strong and medium alternating laser. Sandwich structures are found in structures that are heated by remelting [32].

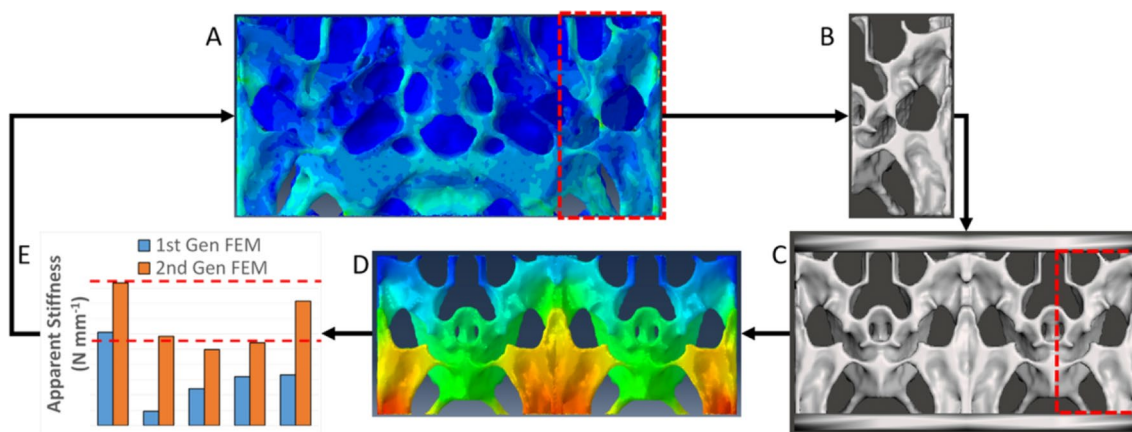


**Fig. 3** **A** Unit cell encompassing regions with maximum energy storage, **B** Second generation unit cell, **C** Second generation VBM coupon, **D** finite element model, **E** experimental quasi-static compression outcomes; dashed red lines show lower and upper EVA stiffness constraints [18]

The tomographic procedure is shown in Fig. 10. AM tomography method is used to control the polymerization kinetics [33].

AM is involved in the development of micron orthogonal crosslinking mechanisms with innovative architectures. In these mechanisms, dual silicon lattice (SiLDNs) can report photos and the formation process (3D printing) [34]. Electrohydrodynamic jetting uniquely permits the generation of submicrometer jets that can reach speeds above 1 m/s, and trajectory can be continuously adjusted with lateral accelerations up to  $106 \text{ m/s}^2$  [35]. In structures, to reduce the torque and mass of inertia, the lattice structure can be used in the design of the compressor. The lightness of the blades leads to improved transport in aircraft [36]. In AM method, the NiAl-(Cr, Mo) nanocomposites are used for high solidification rates [37].

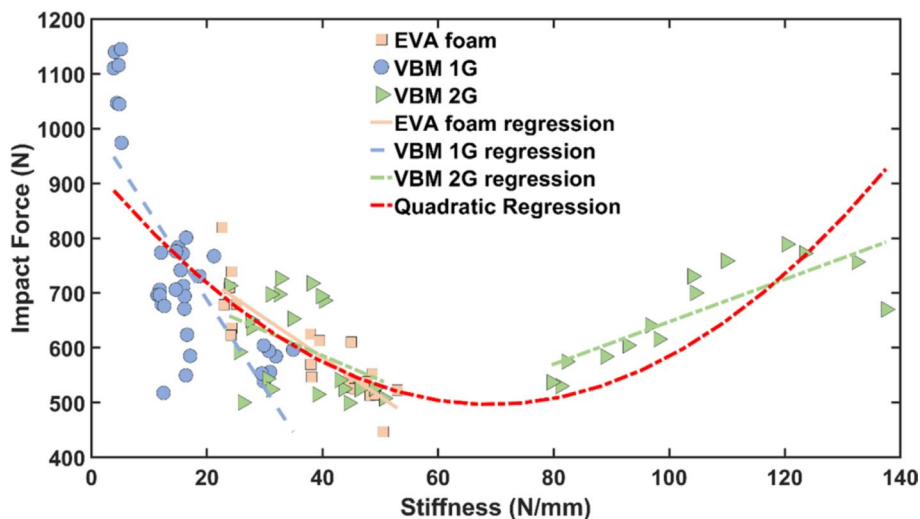
Friction stir additive manufacturing (FSAM) is a suitable alternative to AM to obtain excellent mechanical properties.

The FSAM technology utilizes metal additive manufacturing (MAM) to improve mechanical and microstructural properties. FSAM process is an appropriate option resulting in excellent mechanical attributes with refined grain structure of the build layer [38]. However, some research works to prove a decrease in microhardness because of small-scale porosity and the cavity [39–42]. With easy AM techniques such as 3D printing, shadow masking, and PDMS molding, 3D-printed, modular, electrochemical sensor-integrated transwell systems have been demonstrated for monitoring molecular and cellular events in situ [43].

To design MMC microstructures and evaluate laser beam defocus performance, a multi-beam LDED is used [44]. The cooling rate depends on the Laser powder bed fusion (LPBF) process parameters and correlates these cooling rates to the final material-based MAM [45].

Stacking fault energies (SFE) have been obtained in AM stainless steel (SS 316 L) and equiatomic CrCoNi

**Fig. 4** Impact force in terms of stiffness regressions. 1st- and 2nd-generation VBM data were gathered to get for the quadratic regression [18]



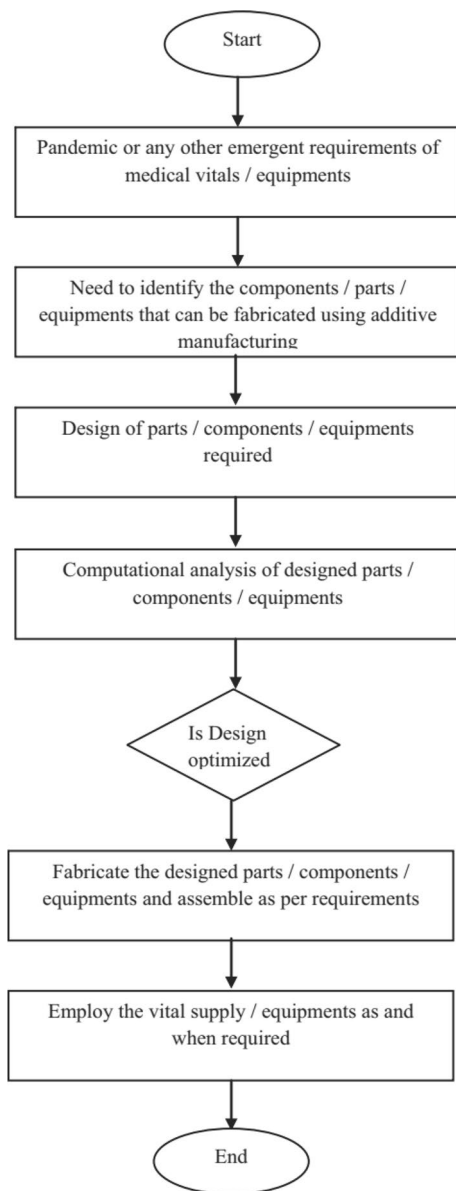


**Fig. 5** Flowchart of the process of using AM in response to this epidemic [21]

medium-entropy alloys [46]. In alloy models, complete grain transfer can be achieved using a high-intensity ultrasound. To investigate this transfer, the laser powder deposition method is used. For example, the use of AM Ti–6Al–4V alloy improves the specimens' yield stress and tensile strength. Compared to the conventional AM columnar Ti–6Al–4V, this alloy increases the mentioned parameters up to 12% [47]. Figure 11 shows the schematic metal AM utilizing a laser-based DED at 20 kHz. In high-intensity ultrasound, the presence of current and the formation of acoustic cavitation stimulate the intensity of the freezing process [47]. The research work [48] has presented the first report of VAM-printed thiol-ene resins.

Figure 12 shows the mechanically adjustable method of thiol-ene chemistry. In these curves, solid lines and dashed lines represent the response of samples to light and the response after heat treatment, respectively [48].

Also, the methods employed in batteries and supercapacitors, energy storage materials, electrolytes, etc., can be examined by 3D printing [49]. In Ni-based superalloy, a novel and different HT protocol has been designed to satisfy the requirement of "no RX together with uniform  $\gamma'$ ". It is possible to use dislocation rearrangement and annihilation, otherwise inactive in the absence of rafting  $\gamma'$ . The obtained results open a path to create single-crystal superalloy AM [50]. A new method has been proposed for the 3D printing of transparent ceramic structures. For example, in Nd-doped yttrium aluminum garnet (YAG) structures, by two-photon printing, undergo photopolymerization and the sol–gel process (see Fig. 13) [51].

In comparison with commercially available elastomer resin printing, LCE structures printed with 3D printing are 12 times slower and suffer from 27 times more strain-energy loss [52]. A set of nitrogen-bonded carbon–metal structures can also be introduced as strong additives for 3D printing inks. These additives (like  $N\text{-STC}/M_xO_y$ ) are very important for making mesenchymal stem cells [53]. A different platform technology has been introduced that enables 3D and cross-laser printing of PEG-based materials [54]. The spine of polyester-containing materials can be easily corrected and destroyed with this technology generally [55].

In tertiary recycling, materials may be recycled while maintaining stability. Consequently, Comparatively, to primary and secondary recycling methods, this recycling can be considered economic. In this type of recycling, a solvent is used to recycle thermoplastic materials. This type of recycling is also used in thermal cracking, gasification, synthetic fiber reinforcement, hemolysis, and thermal energy production. Finally, the incineration process is introduced as the quaternary recycling process. Due to high pollution, this method is considered a danger to the environment [56]. The basic recycling processes are shown in Fig. 14.

Mechanical properties have been analyzed of selective laser melting manufactured AlSi10Mg aluminum compared and alloy with sand and gravity die-cast AlSi<sub>10</sub>Mg parts [57]. Also, a high level of residual stress and metallurgical defects commonly happen in SLM-fabricated aluminum alloys. But explaining the above defects' formation mechanism is imperfect (see Fig. 15) [57].

Wire Arc Additive Manufacturing (WAAM) is a modern method of producing metal components [58, 59]. In this technique, large metal components are created layer by layer. Specifically, the research will focus on screw-feeding setups with microstructure, hardness, grain size, and reinforcement ratios of manufactured reinforced materials "composites" [58]. The advantages of this method include minimizing

**Fig. 6** The schematic figure of the 3D bioprinting steps [25]

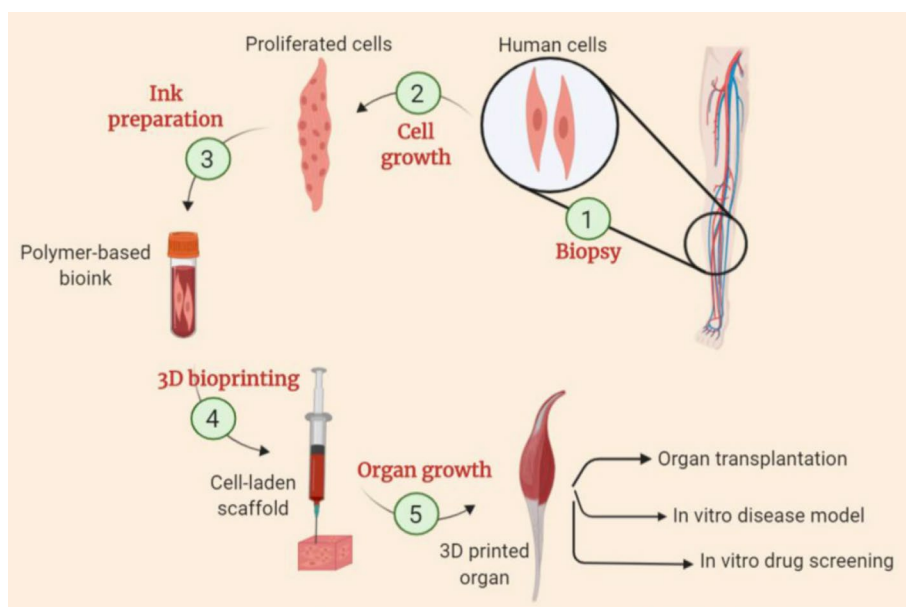
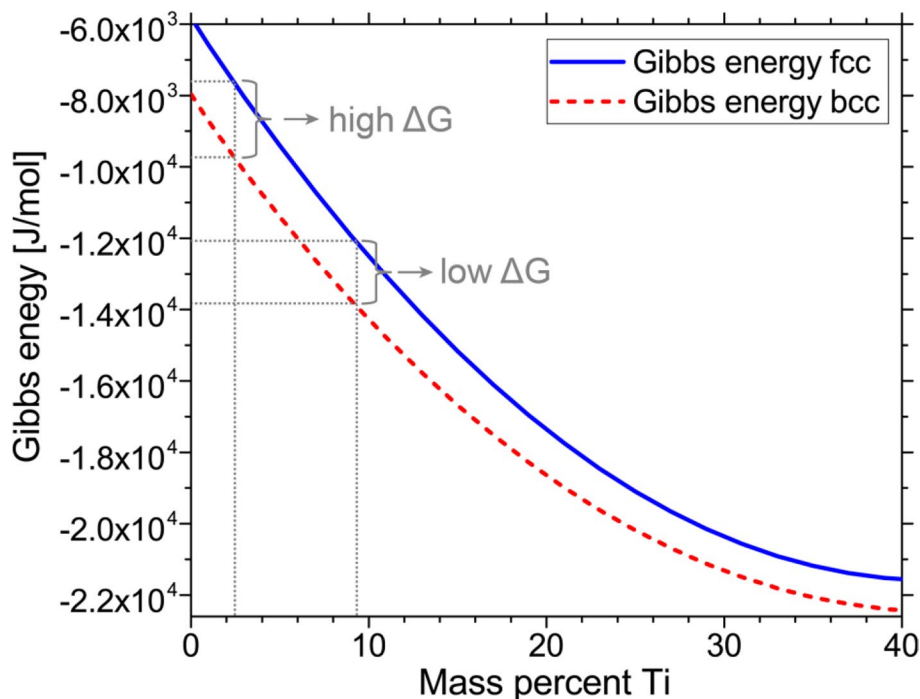


**Fig. 7** Thermodynamic estimation of the driving force for martensite formation [29]

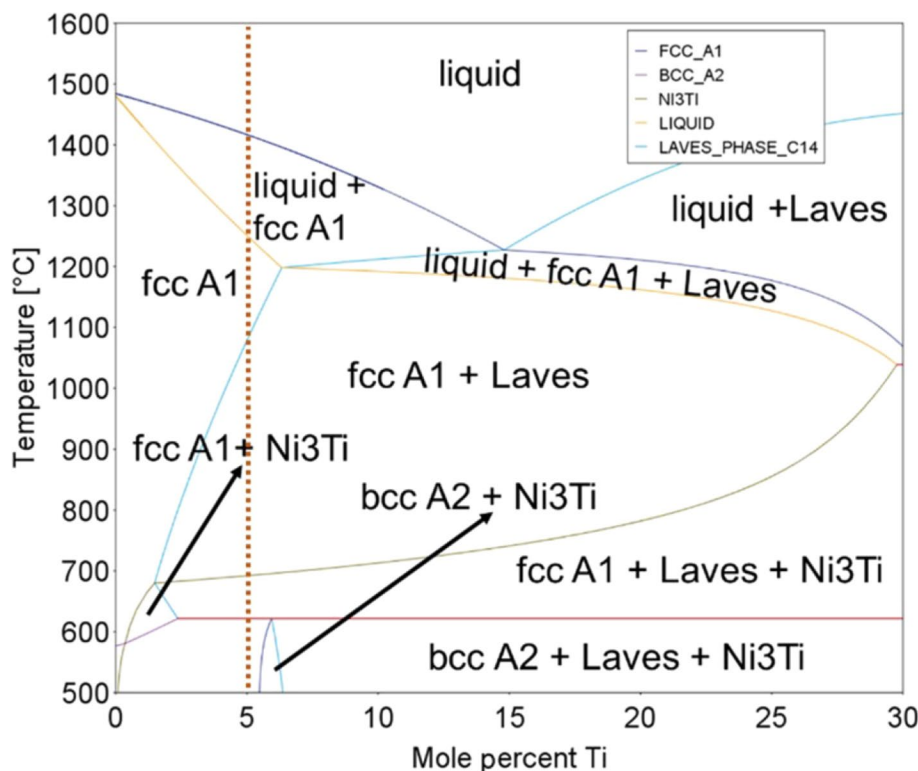


wire contamination and identifying any defects. This method is widely used in the aerospace industry [58]. Another study [59] has been reviewed to bridge the knowledge gap about reviewing commercial and proficient aspects of the widespread application of WAAM [59–61] in some industries. In this research, the capabilities and implementation steps of the WAAM method have been investigated [59]. Figures 16 and 17 show that the WAAM method can also be used for crane hooks [60].

As a result of the WAAM method, Huisman can manufacture components with complex shapes, local alternative material properties, or short delivery times, improving corrosion and wear resistance, for instance [60]. Additionally, there are several procedures under the AM technology; Fig. 18 [59] categorizes some essential AM procedures. The following subsections give brief details of these procedures.

Part fabrication utilizing WAAM involves Process planning, deposition, and post-treatment. Figure 19 represents the series of steps of fabricating a part [59]. LAM is a group

**Fig. 8** Pseudobinary phase diagram for the Fe<sub>19</sub>Ni<sub>1-x</sub>Ti<sub>x</sub> (wt%) alloy [29]



of processes that are rapidly gaining popularity across a variety of industries. Using a laser beam, a substrate is melted and then the material is added to the melt pool. As a result, a very localized zone of material is deposited. In biomedicine and clinical applications (implants and scaffolds for bone regeneration), this technique is used. By using a cool supersonic gas flow, cold spray deposition speeds up the bonding of solid particles to substrates [62–69].

Metallic sheets are used as feedstock in sheet lamination SL or laminated object manufacturing LOM. Generally, a 3D object is formed by using a localized energy source, usually ultrasonic or laser.

Also, wire arc additive manufacturing WAAM is defined as a typical production process employed for 3D printing or repair of metal parts. It is related to the Direct Energy Deposition DED group and family of Additive Manufacturing AM processes. That is, arc welding-based additive manufacturing or wire arc additive manufacturing WAAM methods and techniques are interesting for the manufacturing industries due to their potential to manufacture big metal components with low cost and short production lead time typically.

AM is a stable method for producing customized DLA. For several rods or walking sticks, the same workflow could be used for an elbow crutch [71]. Also, a general idea of multi-material in conjunction with reinforced material field creation by changed AM has been done [72]. The research work [73] proves the main similarities between fusion-based AM and fusion-based multipass arc welding, particularly

solidification mechanisms, thermal effects and chemical reactions within the melted region, and residual and distortion stresses. In one study, AM was used to optimize processing parameters. In this method, three energy, geometric and thermal criteria are used to obtain the optimal distance of processing parameters. The determined results show that the analytical values of the valve distance are associated with a high limit. This high limit can be useful in setting method parameters such as travel velocity, strength, and layer thickness to determine the defect. The following equation calculates the energy density (ED) of the system,

$$ED = \beta \frac{P}{v h d} \tag{2}$$

here, P, h, v, and d represent power, hatch distance, travel velocity, and layer thickness, respectively. And  $\beta$  is defined by the following relation (Eq. 3):

$$\beta = \frac{g_s}{d_{Heat\ Source}} \tag{3}$$

here,  $g_s$  and  $d_{Heat\ Source}$  represent the powder grain size and heat source diameter. The used physical quantities (for power/energy calculations) considered in AM mathematically are reported in Table 1 [73].

It is significant to highlight and note that both end passes (1 and 4 in Fig. 20a) contribute with just only one-half each to



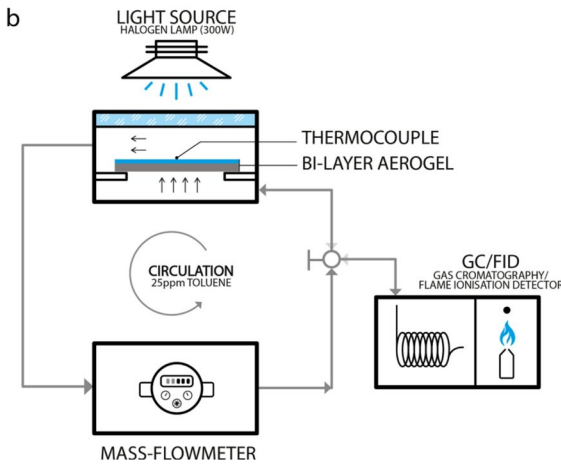
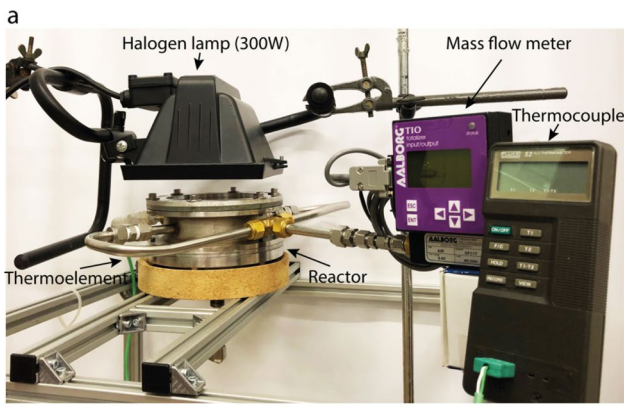


**Fig. 9** VOC degradation system and Light-driven gas pump **a** working scheme and **b** setup [30]

the energy balance. The following equation calculates the heat input for AM (3D-printing) [73],

$$HI_{3D} = \frac{Energy}{Volume} = \frac{Number\ of\ passes \times Energy\ per\ pass}{\Delta x \times \Delta y \times \Delta z} \tag{4}$$

Presentation of the methodology used to obtain the maximum theoretical hatch distance for the three proposed criteria is as the following (revisiting fundamental welding concepts to improve AM: From theory to practice; see Figs. 20b, c) [73].

$$h \leq h_{max} = \sqrt{R_m^2 - Z_{powder}^2} \tag{5}$$

In which,  $Z_{powder}$  is user-defined. Also, there are three proposed criteria for  $R_m$  as the following,

1. Geometric: Determined experimentally

$$Energetic: R_m = \sqrt{\frac{2P}{\pi v (C_{Psolid} \Delta T_{solid} + Heat_{fusion} + C_{Psolid} \Delta T_{solid})}} \tag{6}$$

- 2.

$$Thermal: = T_0 + \frac{P}{2\pi KR} e^{\left(\frac{vR}{2a}\right)}, \text{ when } T = T_f \rightarrow R = R_m \tag{7}$$

- 3.

As a different research work, the manufacturing of a diversity of magnetic materials utilizing different AM methods has been reviewed in the reference of [74]. In this study, two methods of large area and AM connector have been used. This method is used to print bond magnets. AM machines can also be used to print anisotropic hard magnets. These machines are equipped with controlled magnetic bonding devices. Thermal sensors, building platform temperature control, and high-temperature furnaces are among the applications of AM technology. Such integrated systems can significantly accelerate AM application for magnetic material processing [74].

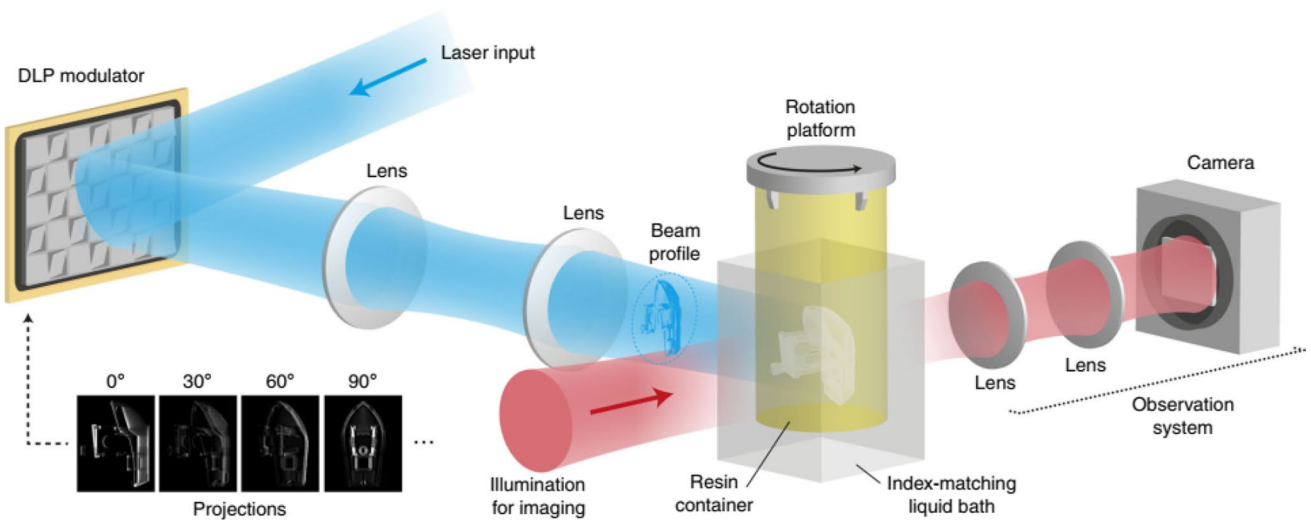


**Fig. 10** The setup used for high-resolution tomographic [23]

**Fig. 11** High-intensity ultrasound during metal AM [47]

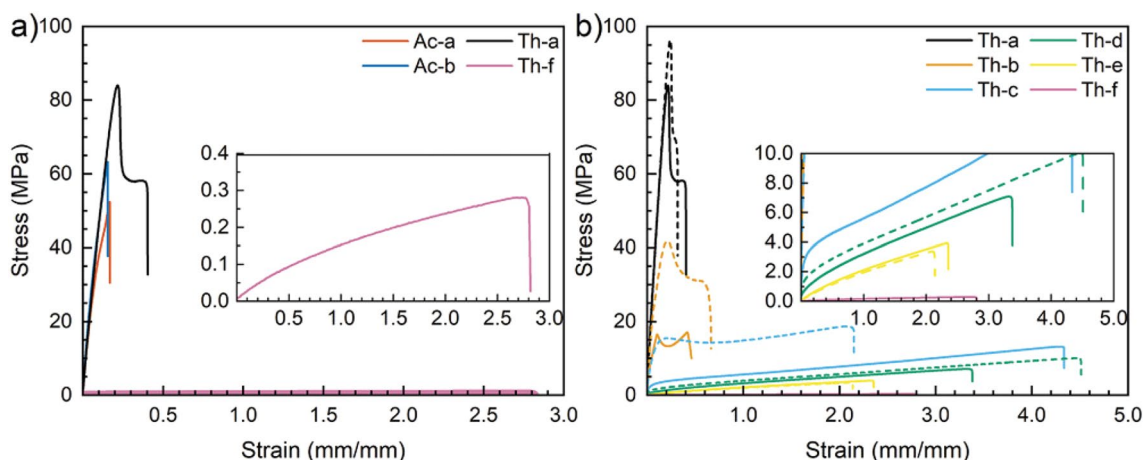
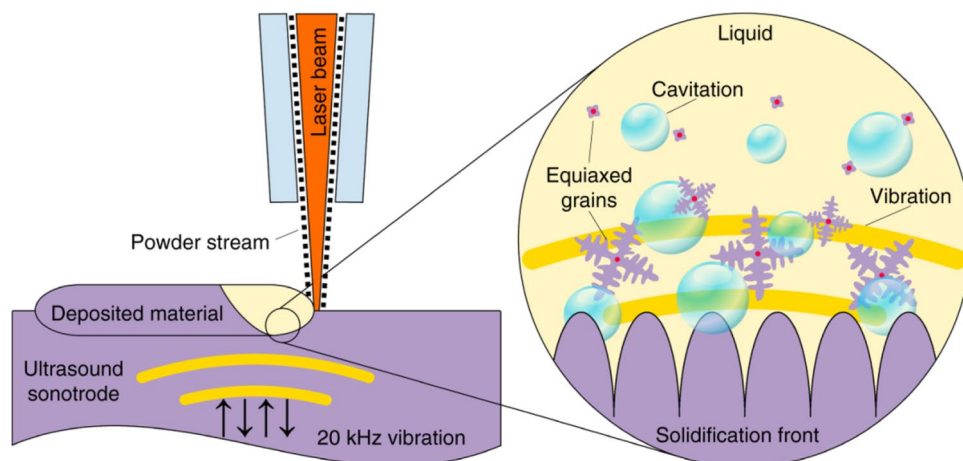


**Fig. 12** Tunable mechanical manner of thiol-ene chemistry. **a** Tensile response of thiol-enes Th-f and Th-a compared with acrylates Ac-a and Ac-b, composed of the same monomers and functionalities. **b**

Screening the full range of thiol-ene compositions presents a broad range of mechanical properties [48]

Generally, four AM techniques, such as Selective Laser Sintering (SLS), Fused Filament Fabrication (FFF), Stereolithography (SLA), and Multi Jet Fusion (MJF), have been investigated [75]. In general, the AM method is very cost-effective due to the lack of tools [75]. Compared to the AM model, the MSF model can calculate fatigue life more logically, and more accurate performance prediction leads to design optimization [76]. One of the main goals of this model is to reduce the time interval between design and certification and production of defective parts [77]. Hence the combination of mechanical fluid flow modeling and appropriately selected experiments in a limited range of AM parameters helps produce more efficient printable data.

Biomimetic designs are very beautiful in terms of beauty and very efficient in terms of application. Therefore, by changing the design strategy, we can observe the growth of gradient technology in a wide range of systems (see Fig. 21) [78].

Researchers have reported that AM printable filaments can have adjustable electrochemical properties [79]. Electrochemical properties can greatly improve the production of 3D / manufactured printed electrodes (AME). The procedure is to use Zn-MnO alkaline batteries to apply the potential (about 1.5 V). There is oxygen gas in the battery anode and hydrogen gas in the battery cathode. The FFM / polymer AM filaments produced are used for water-splitting. The use of this potential method leads to the reduction of expensive electrocatalytic nutrients. It is therefore possible to maximize the benefits of AM by redesigning the electrode structures. In research work, this potential was investigated in many AM disciplines by changing their composition in the intended application [79]. A schematic representation of the composition of additives in PLA is shown in Fig. 22.

A series of calculations and experiments have been presented that targeted addressing the problem mentioned above. Three-point bending tests have been used to

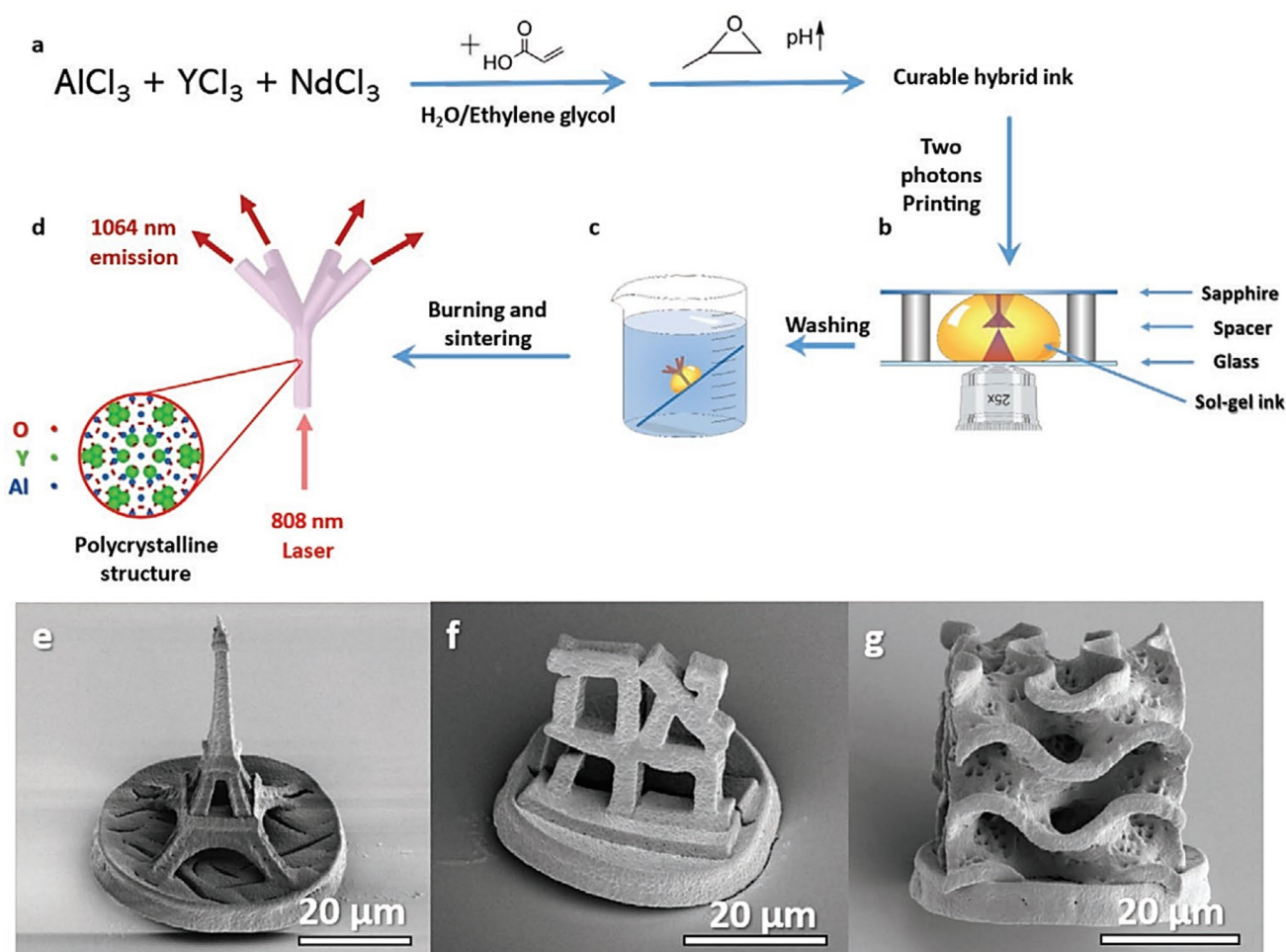


**Fig. 13** Scheme illustrating the preparation of doped YAG 3D structure **a** Starting from metal salts dissolved in ethylene glycol and water together with acrylic acid, followed by the addition of PO at the second stage **b** At the next stage, the printing of the ink using a two-

photon printer on top of a sapphire base was performed **c** followed by washing the obtained 3D object **d** Final heating at elevated temperature was performed to form single-phase Nd: YAG **e–g** Printed polycrystalline structures after heating to 1500°C [51]

characterize cementitious samples. Molecular dynamics (MD) simulations and quantum density functional theory (DFT) calculations can be used to investigate and predict the surface chemical and mechanical interactions of different materials. By combination the theoretical and experimental methods, the diverse properties of structures may be estimated truthfully. An interlayer area of two successive layers of printed cement was studied to determine the effect of a cohesive additive. The results of DFT analysis show that epoxy can not only mitigate the harmful effects of interlayer water. But also, drastically changes the nature of the interactions in the area between the layers (see Fig. 23) [80].

To produce 3D-nano-architected titania with a submicron resolution, an AM procedure has been developed. Also, the efficiency of this procedure has been explained by utilizing woodpile FCT architecture with individual feature widths of 150nm as a model system [81]. A novel plan has been proposed to generate tailored polymer- and composite powders

with defined high flowability and composition. Polystyrene/silica ( $PS-SiO_2$ ) has been used as a model composite system and focuses on the in-depth characterization of the formed supra-article powders for size, morphology, distribution, and composition [82]. Figure 24 represents the dispersion of silica additives dispersed in specified proportions of the printed sample.

The gravitational fiber drawing (GFD) method can develop precisely organized nanostructured materials by the bottom-up approach, polymers and solvent systems, simple manufacturing procedures, and scalability advantages. The figure of the nano-fiber handling, gravity-drawing experiment, scaffolding device, and PCL-GFD fabricated nano- and microfibers are depicted in Fig. 25. With some revisions in the scaffolding instrument, it is simple to coil or wind the fiber around various geometries [83] (see Fig. 25).

Research has been conducted on the use of recycled polymer in AM. The application and use of recycled materials

**Fig. 14** **a** Thermoplastic recycling procedure for waste management by mechanical and thermal means **b** Waste management hierarchy **c** Tertiary and quaternary recycling procedures [56]

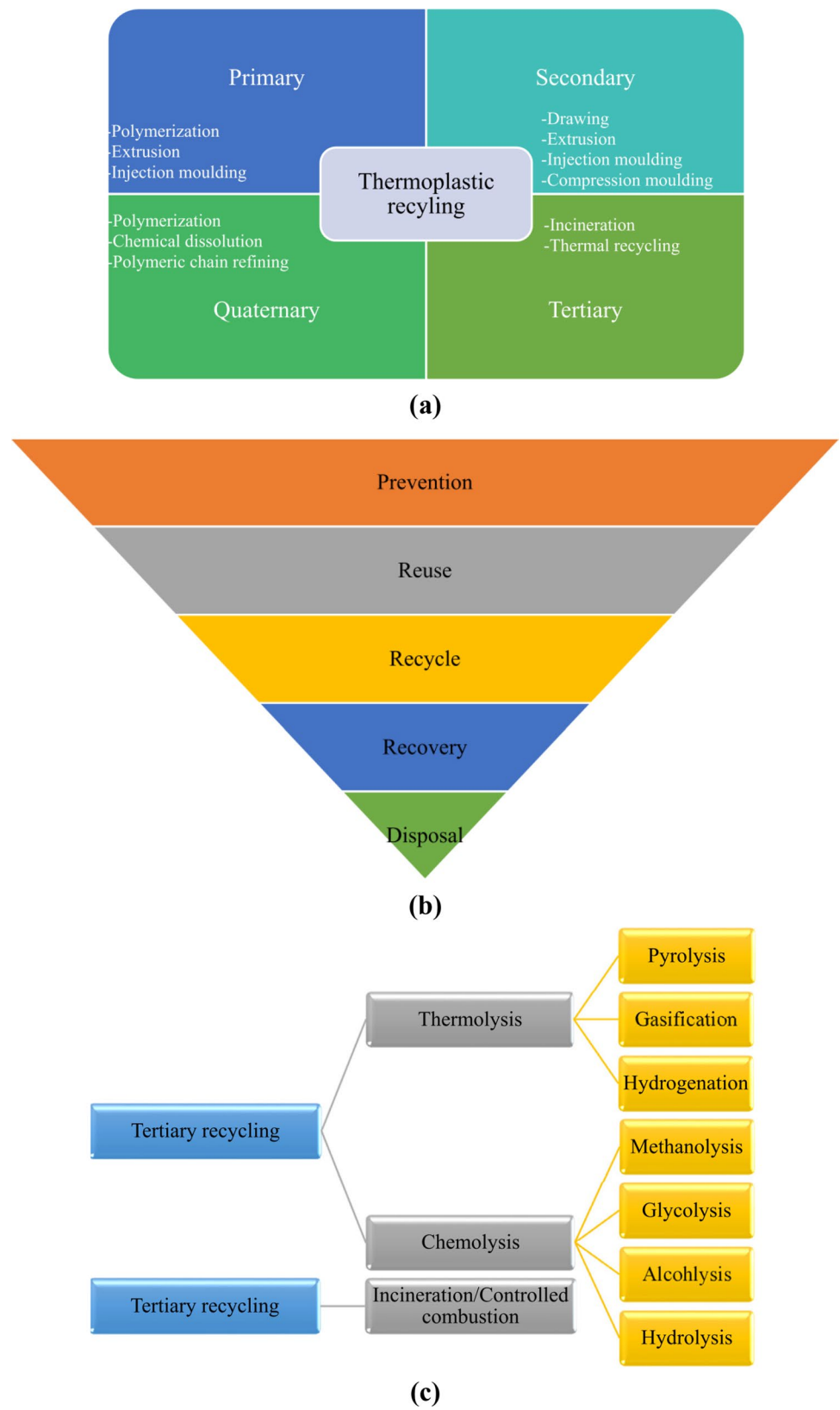


**Fig. 15** Stress–Strain Curve of AlSi<sub>10</sub>Mg Samples (from experimentation) [57]

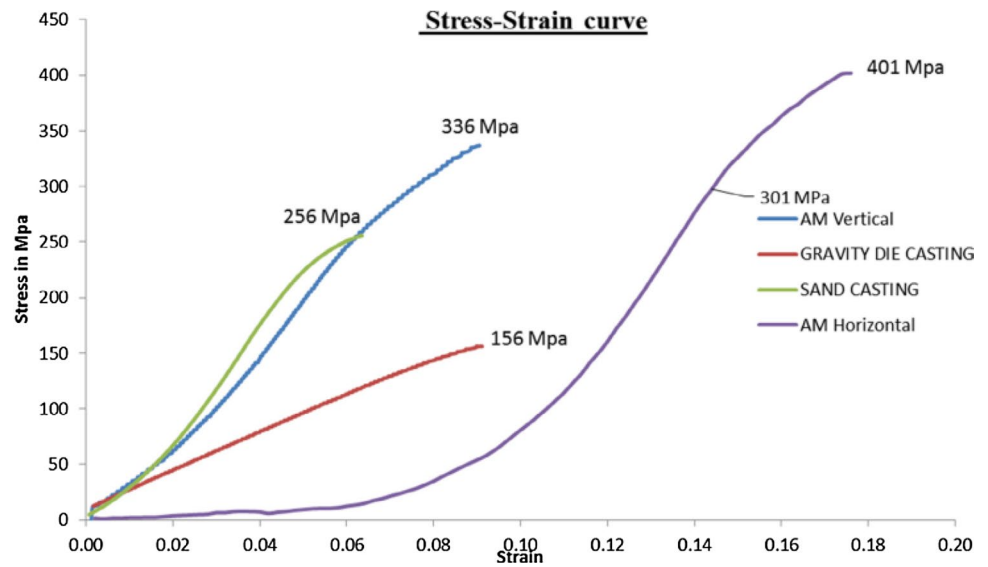


**Fig. 16** HUISMAN'S 3D printed WAAM hook [59, 60]

in the FDM (Fused Deposition Modeling) will contribute to a major development. Polymer waste disposal involves different approaches, but recycling polymer is an effective method. FDM is a low-cost AM technology that uses thermoplastic filament to build layers of parts. The evolution of FDM leads to the enhanced use of recycled polymers for diverse applications. To manage polymer wastes, FDM can be used. However, understanding the performance of recycled polymer products produced through AM is essential [84, 86]. Figure 26 displays the procedure involved in converting plastic waste into filament subsequently processed as 3D printed products.

Utilizing processing approaches, cavities may be prevented, and fiber and matrix interference may be enhanced. The chances of composites forming defects and having decreased strength are high in AM. The FDM technique is



**Fig. 17** HUISMAN'S 3D printed crane hook [60]

the most potent method for developing fiber composites, decreasing the composite processing price and time [85, 86]. Electrostatically exfoliated two-dimensional layered materials can be additively manufactured to make intricate layouts [87]. The outcome is the 3D/3D vdW mono- and heterostructures that are mechanically electrically conductive, robust, and electrochemically active over a broad pH range and even radiation tolerant. A flexible workflow has been showcased to fabricate inertial microfluidic devices for both industrial and experimental applications. In addition, a novel inertial microfluidic device with a right-angled triangular cross-section has been fabricated and examined, which

**Fig. 18** Categorization of essential AM processes [59]

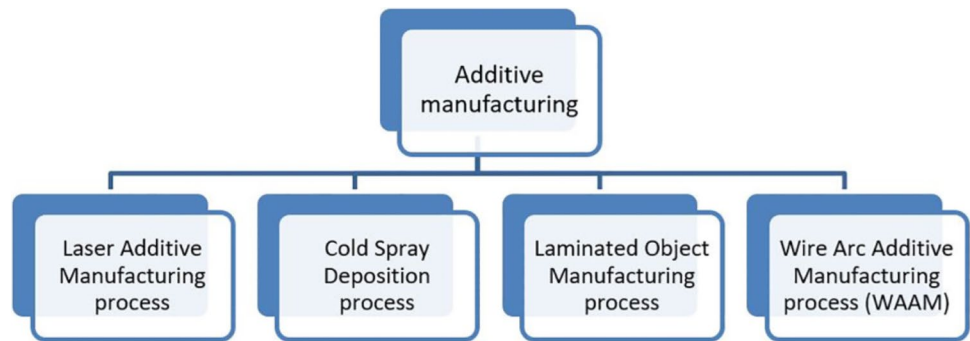
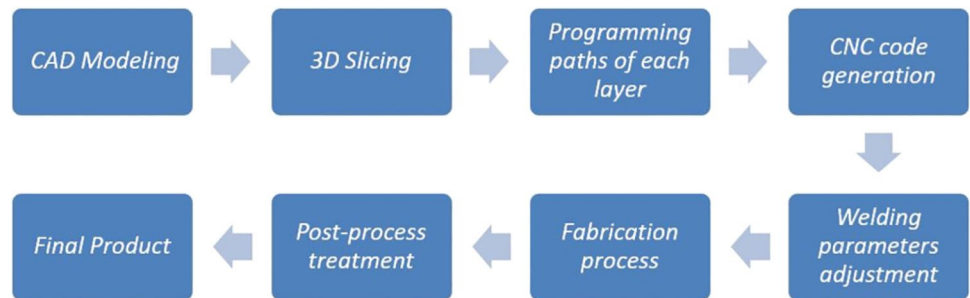


**Fig. 19** Categorization of essential AM processes [59]



is analytically infeasible to manufacture by photolithography [88]. AM has been used to process Fe–Ni-based alloys [89–95]. For example, the research work [92] has presented a novel method for manufacturing fccFeNi alloy employing AM.

Using the WAAM method, it directly produced iron-nickel alloy and studied the structural properties of its bulk materials by studying its neutron diffraction. In this technique, owing to the intense thermal input of the sediment, re-melting/freezing cycles lead to the formation of large grains of this alloy. C/a ratio analysis further characterize the dissolution process of FCC-FeNi anisotropic superstructures from 706 °C heating to 616 °C cooling. The TECs of the WAAM fabricated FeNi during cooling and heating are estimated utilizing the lattice thermal volumetric strains. The results showed that the thermal operation causes the

anisotropic dissolution of FCC-FeNi and thus the defect in the bulk material FeNi [92].

Nowadays, many researchers use efficient AM methods to produce and study metal structures. This method and technique support economies such as linear and circular economies. As part of a circular economy, the supply chain needs to be rebuilt and broken in the same places where AM requires it. Moving from a linear economy (Fig. 27) to a circular one (Fig. 1) is like chaos. But the chaos needed to run sustainable production is similar to what AM needs and promises similar profits [70–102].

Newly researched works and markets published a study of the AM's market applied to the aerospace sector. Recent predictions prove and show the complete potential of 3D-printing and AM technologies in aerospace and other applications. Several applications of AM have been found in industrial societies for some time now. For example, AM is applied in aircraft manufacturing, helicopter sections, making lighter and more effective engines, 3D-printed turbines, some hooks, etc., 3D-printing technologies usually save on cost, time, and money and make stronger, more efficient finished products correctly. The research works and markets studies and investigations prove that. AM in aerospace and other engineering industries is now growing and increasing. It should be mentioned that AM technology has vast and enormous applications in the aerospace industry [103–105].

A concept of the applicability of composite AM has been introduced to morphing aerospace structures (Figs. 28, 29). It represents the first significant effort toward producing composite morphing structures in an automated,

**Table 1** Summary of the major equations for power/energy estimations in AM [73]

Description	Mathematical equation
Linear heat input ,J/mm	$LHI = \frac{P}{v}$
Effective energy per unit of area,J/mm <sup>2</sup>	$E_{eff} = \frac{P}{vd_{Laser}}$
Energy density or volumetric fluency, J/mm <sup>3</sup>	$F = \frac{t_{imp} P}{h d o}$
Energy density, J/mm <sup>3</sup>	$ED = \frac{P}{vhd}$
	$ED = \frac{P}{\rho_{bed} d_{Laser} h d}$
	$ED = \frac{P}{\rho_{bed} d_{Laser} h d} \left( 2 - \frac{h}{d_i} \right)$
Power deposition density,g/mm <sup>2</sup>	$PDD = \frac{R}{vd_{Laser}}$

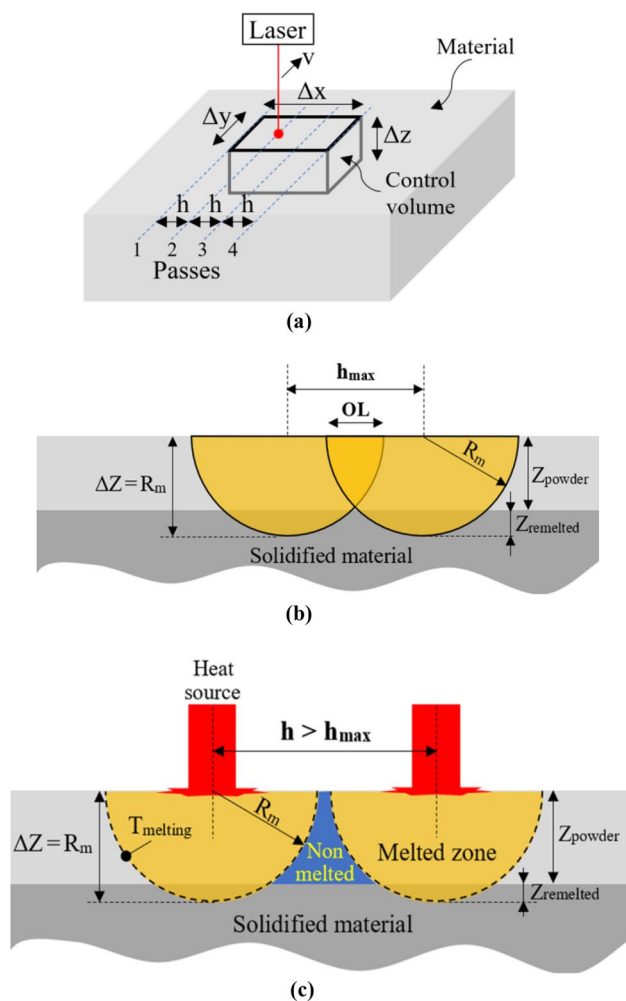


**Fig. 20** **a** Control volume employed to obtain the in-volume heat input (energy density) during additive manufacturing (AM). **b** Geometrical profile created by two consecutive melted tracks in AM where melting of the powder and partial remelting of part of the previously deposited layer occurs. **c** Schematic representation of a non-melted region if the hatch distance,  $h$ , is higher than the maximum allowed hatch distance,  $h_{max}$  [73]

cost-effective manner. On a 2 m wingspan example, greatly enough controllability may be obtained by exploiting the proposed design and manufacturing idea. The possibility of automating the process and waste-free manufacturing indicates a vast potential for cost-effective aerospace structures. This is enabled by exploiting the compliant mechanism concept, relying on flexible structural members in place of hinged structures [103].

The camber-morphing idea is according to the conception of distributed compliance and electromechanical actuators. The concept of the compliant rib is depicted and presented in Fig. 28. Also, the idea and the final drone are depicted and shown in Fig. 29.

AM (and 3D printing) is an innovative manufacturing method. It is expected to reform the future of

manufacturing industries. In contrast, different materials are employed in AM. As a result of its ability to produce high-strength structural components, AM metal is expected to have a significant impact on the industry. Nevertheless, defects happening in metal AM prevent the method from extensive adoption by the major industries [106–109]. To evaluate, analyze, and verify these defects correctly, they must be evaluated, analyzed, and verified. Defect evaluations [106], defect prediction [107], and defect detection in the AM materials are very vital, required, and important [108, 109].

So far, ultrasonic testing (UT) methods have been used to detect defects in engineering components. Advanced UT methods such as laser ultrasound (LU), step array ultrasonic testing (PAUT), and guided waves have shown potential in AM product testing. UT techniques emphasize the use of the AM method to assess damage and defects in products and to test raw materials such as powders, wires, and filaments in additive manufacturing [106]. An in-depth analysis and investigation of these materials are needed before testing. It is, therefore, necessary to investigate on-line UT techniques for different parameters such as defect size testing, test sample geometry, defect depth, and elastic properties of wires and filaments used in AM processes [106]. A new and widespread part-scale thermal form and modeling for defect prediction are introduced for powder bed fusion fabrication. Utilizing the principle of superposition POS (Fig. 30), the temperature field owing to a moving power source can be precisely calculated at the component scale with no temporal or spatial decreasing of the model. That is an essential step toward the final objective of strongly predicting build defects at the part-scale [107].

A single scan across the surface of a 5 mm × 5 mm × 2 mm block of Ti–6Al–4V has been simulated and depicted in Fig. 31. The superposition thermal modeling method for part-scale thermal defect prediction, is summarized in Fig. 32. This flowchart has been illustrated via simulation of the V-22 osprey nacelle link PBF fabrication.

Also, the simulation results in 3D maps of the spatial distribution of cold and hot thermal errors (Fig. 33). A simulation temperature and experimental single-scan research are used to predict the number of errors during the simulation generally. As shown in Fig. 33, the spatial distribution of such errors is highly dependent on the location within the component [107]. It should be mentioned that the probability distributions along with their bar diagrams for hot and cold errors have been depicted and shown in Fig. 34.

The  $\phi$  parameter relates local geometry to the probability of thermal errors. So, by using Eq. 8, we can predict the distribution of thermal defects in real components without fully implementing the thermal model. The results show that

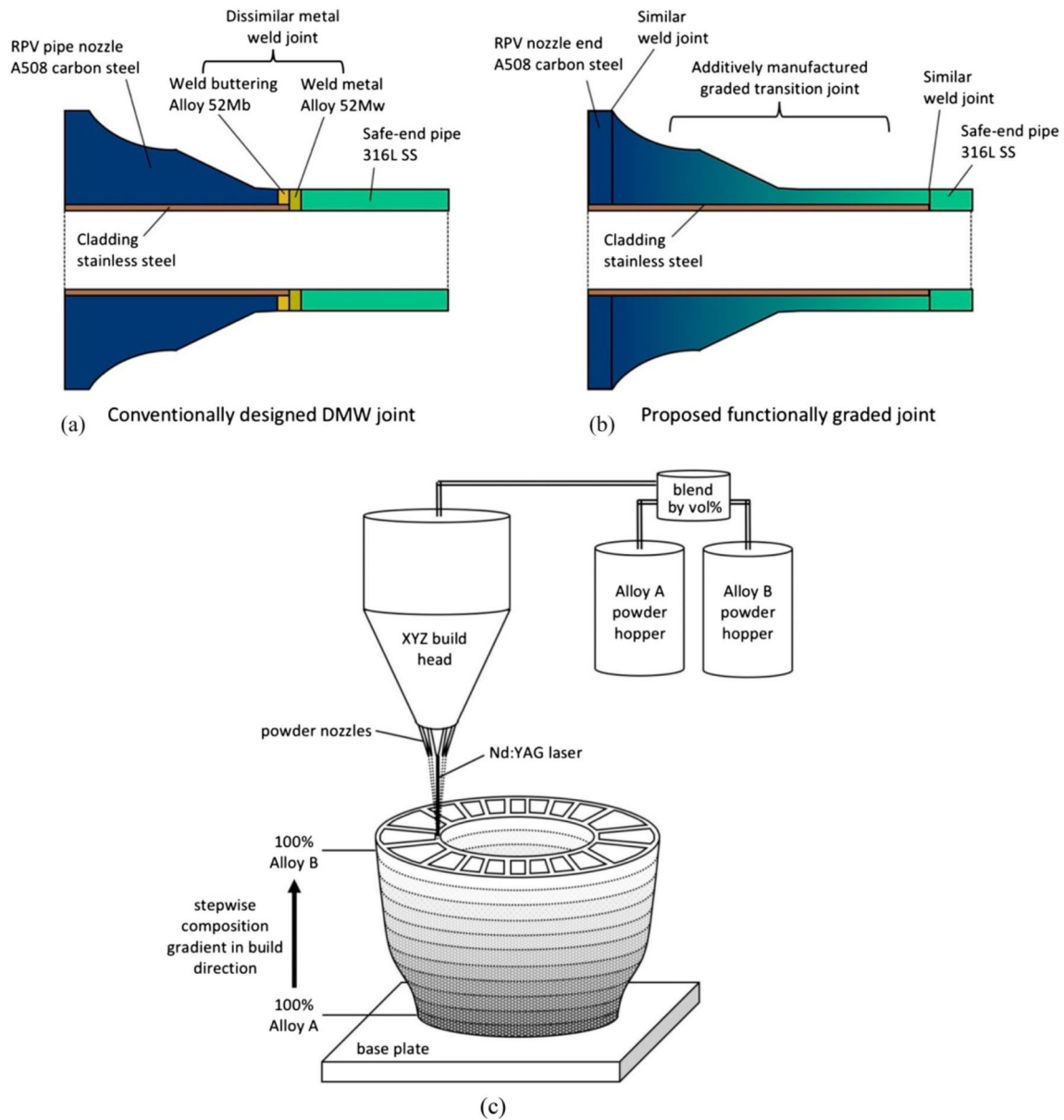


**Fig. 21** **a** Cross-sectional schematic of a conventionally designed dissimilar metal weld joining a carbon steel nozzle with austenitic stainless-steel piping **b** Proposed design for replacing this joint with

a functionally graded insert. **c** Schematic of a laser deposition system with multiple powder feeders can produce a complex geometry part containing a stepwise composition gradient in the build direction [78]

the 1D beta function has the best performance (Fig. 34a, b) [107].

$$P_E(\varphi) = C_0 \frac{\Gamma(\alpha + \beta)(\varphi^{\alpha-1})(1 - \varphi)^{\beta-1}}{\Gamma(\alpha)\Gamma(\beta)} \quad (8)$$

In which,  $P_E(\varphi)$ ,  $\alpha$ , and  $\beta$  represent the probability of thermal errors and shape parameters. Equation 8 provides the first method for forecasting build defects and/or optimizing build parameters. It is very accurate to calculate the error distribution using the parameters specified in the

above equation. An example of these computed parameters is shown in Table 2 [107]. All samples show a calculated error greater than 0.81 in all samples. Consequently, this method may determine several parameters properly.

Future work will address the characterization of the true build history of a real part, the variability/repeatedly of defect populations in real PBF builds, and the characterization of defect populations. A future study will examine how to identify overheating defects more effectively from the linear model [97]. As a final helpful research work, the reference of [110] presents a full argument of the performance



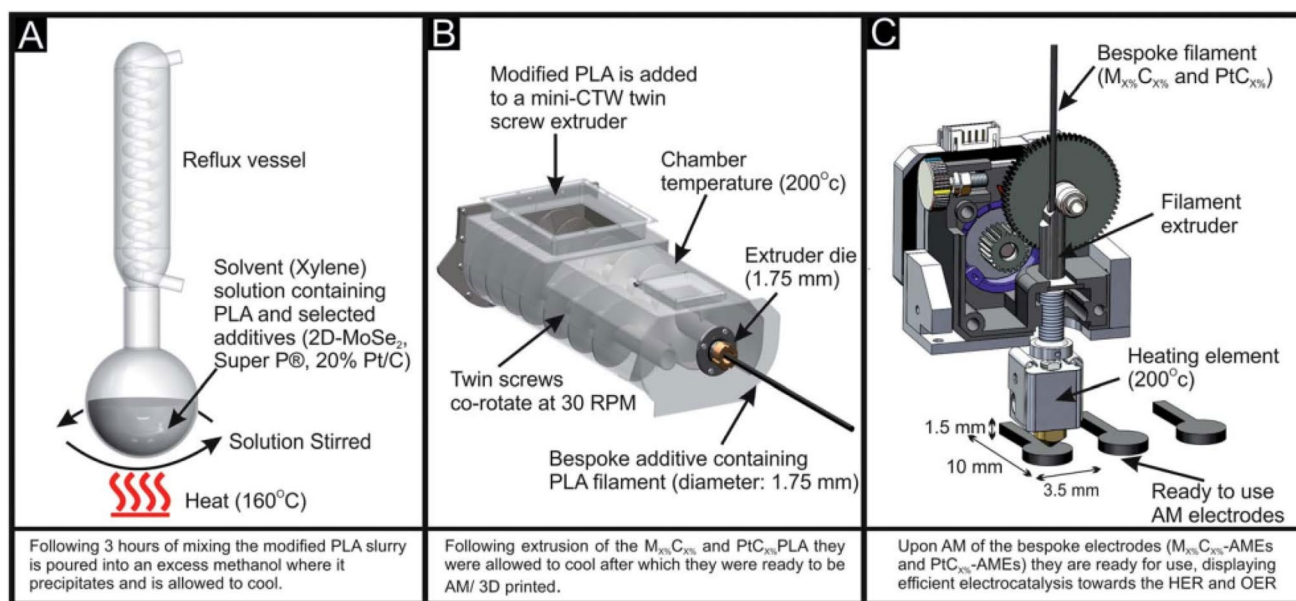


**Fig. 22** Schematic displaying the incorporation of the additive materials within the PLA **A**, the extrusion of modified PLA into a filament that can be additively manufactured **B**, and the AM of ready-to-use electrodes with bespoke electrochemical activity **C** [79]

of AM steels as a function with exceptional microstructural features. As an outcome, Because AM is capable of fast solidification, which limits the formation of MnS inclusions, it increases the pitting corrosion resistance of these steels.

## 5 Concluding Remarks

This review article has tried to present the highlighted, important and novel results in the field of AM and 3D-printing in the year 2020. Which, interesting subjects were introduced, including “some comments (answers questions) about AM and 3D-printing”, “use of 3D-printing and AM in bio-applications, biomedical and tissue engineering”, and other important applications of AM and 3D-printing like AM in metals, polymers, and ceramics. In addition, the relation between linear/circular economies and AM and 3D printing was presented. The additive manufacturing method (AMM) will convert to the first and the best manufacturing method. According to the industrial needs, standards, and qualifications correctly, future study works could help facilitate the optimization (performance and economy) of material design (the best mechanical characteristics and material behaviors) and AM process. Also, AM and 3D printing are the main basis and key base for future 4D and nD printing technologies. Also, the pandemic of COVID-19 in 2020 showed that the manufacturing process (using AM and 3D printing) is vital. Which can be so beneficial for human life and health. These can be the major reasons and motivations for this

review research work in 2020. Some of the results and conclusions are presented as the following briefly,

- The fatigue performance of AM metals is significantly influenced by defects and microstructural heterogeneity. These effects may be due to changes in scanning speed and strategy, geometry, and structure size. AM defects characteristics have played key roles in AM metals' fatigue performance and should be thoroughly characterized.
- It is imperative to fully understand the characteristics of the additive manufacturing defect to fully understand the fatigue performance of AM metals.
- The relationship between fatigue life and microstructural defects should be expressed using a model based on defect variability. Moreover, fatigue uncertainty and scattering significantly affect important aspects of metal additive manufacturing.
- Phenomenological and semi-experimental models can be used to identify defects. For instance, these models like the Murakami model predict fatigue strength well. The model utilizes statistical techniques.
- Metallurgy engineering societies employ continuous mechanics and bottom-up methods, however, in solid mechanical engineering, top-down techniques are utilized. In general, the application of multivariate modeling and simulations can substitute several complex and expensive experiments. Thus, combining two methods from top to bottom and bottom to top may provide

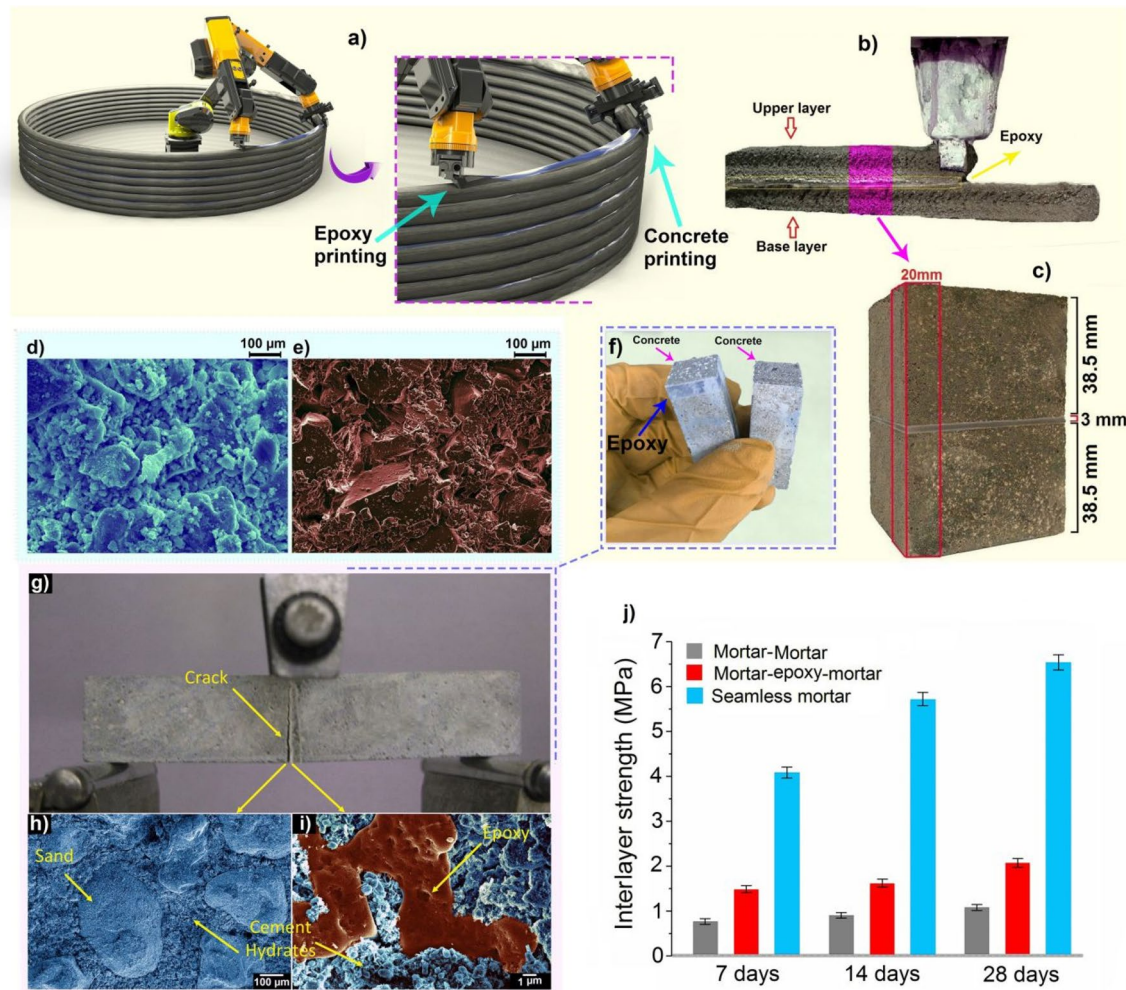


**Fig. 23** **a** Proposed 3D printing device, with two nozzles for mortar and epoxy (concept art) **b** fabricating sample using a conventional 3D printer and the **c** mortar-epoxy-mortar specimen. SEM imagery showing **d** Cement and **e** epoxy surfaces **f** Failed section of the sample **g** mortar-epoxy-mortar sample under loading. SEM image of

the fracture surface of the mortar-epoxy-mortar sample at **h** mortar side and **i** epoxy side, where both contain cement hydrates **j** Tensile strength in the interaction zone for 3D printed of mortar-mortar, mortar-epoxy-mortar, and single mortar block (seamless) specimens at various ages [80]

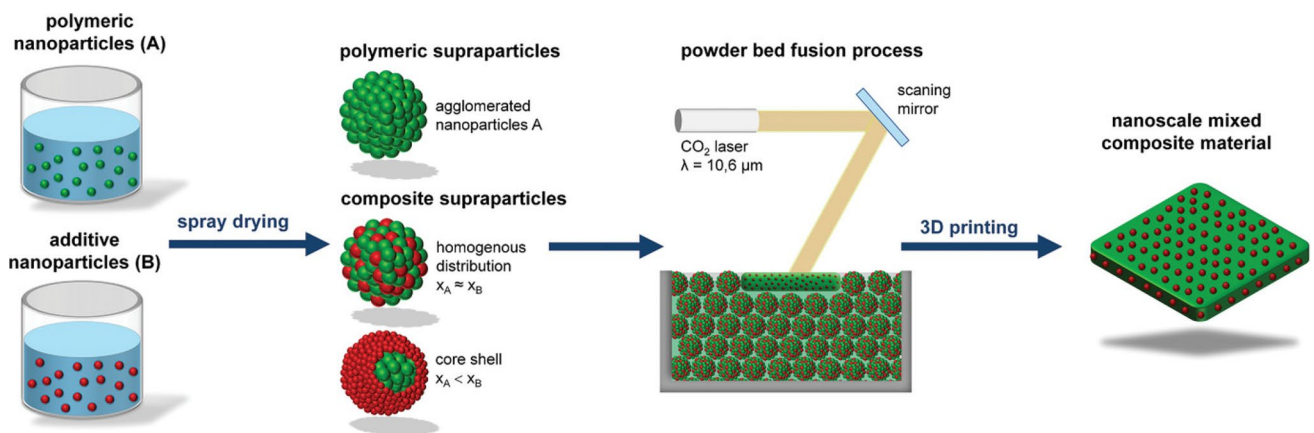


**Fig. 24** Bottom-up fabrication of composite super-particles for selective laser sintering (SLS) [82]

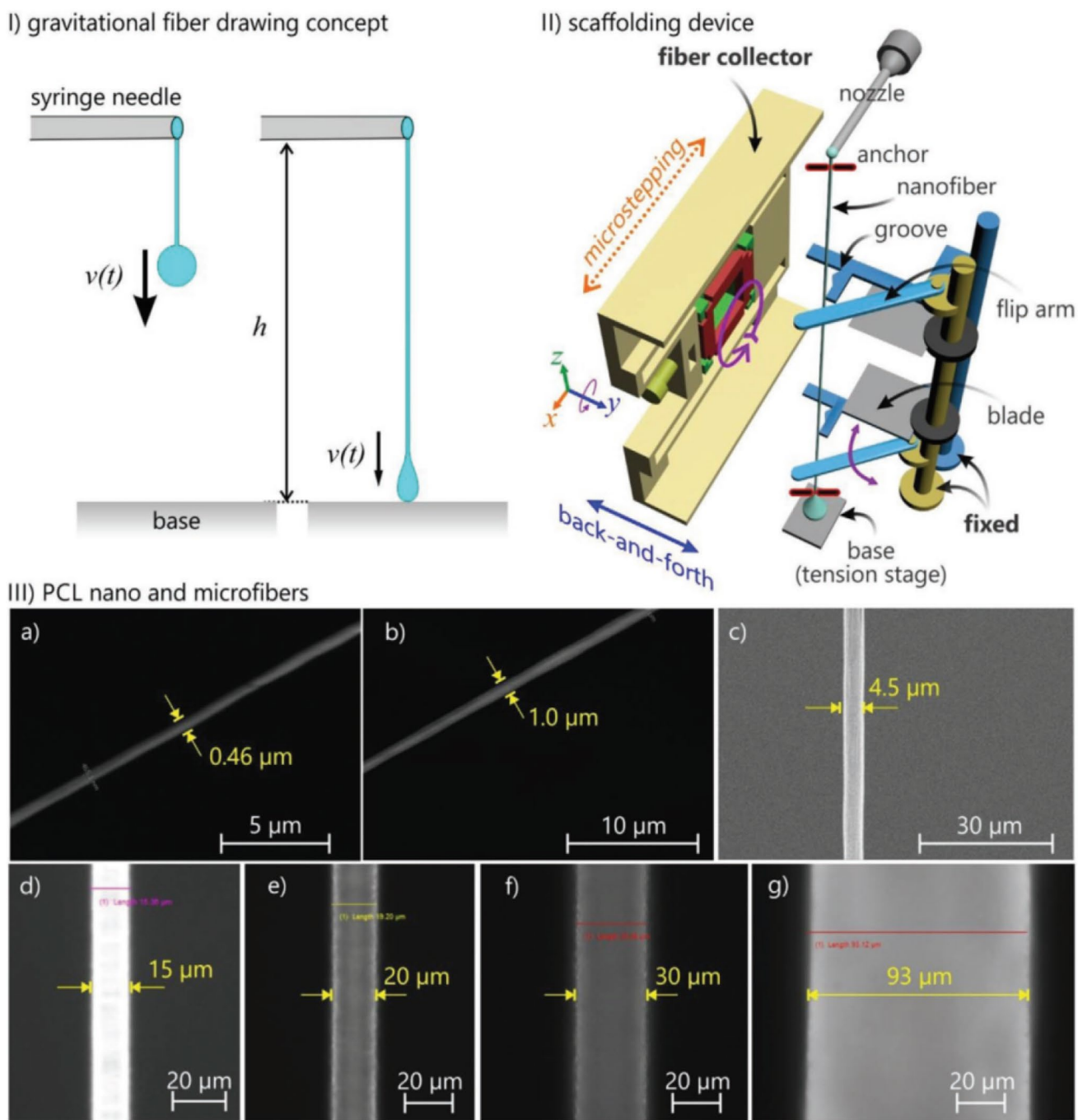


**Fig. 25** I Figure of the gravity-drawing experiment. The droplet falls at speed  $v(t)$ , drawing out a fiber. II Scheme of scaffolding device and nanofiber handling. III GFD fabricated nano- and microfibers of

diameter **a** 460 nm, **b** 1  $\mu\text{m}$ , **c** 4.5  $\mu\text{m}$ , **d** 15  $\mu\text{m}$ , **e** 20  $\mu\text{m}$ , **f** 30  $\mu\text{m}$ , and **g** 93  $\mu\text{m}$  [83]

more precise and quicker performance and eventually enhance product quality.

- In manufacturing, the combination of AI and PES is beneficial for recognizing porosity in AM parts.
- During laser powder bed fusion, different parameters determine the cooling rate. MAM material microstructural features are one of these parameters.
- Ultrasound creating acoustic cavities in the liquid metal increases its melting intensity during solidification because of high-intensity ultrasound. The structure must be fundamentally overhauled or modified.
- The WAAM 3D-printing method was used by Huisman to make medium components (with excellent per-

**Fig. 26** Conversion of waste plastic to 3D printed parts [84]

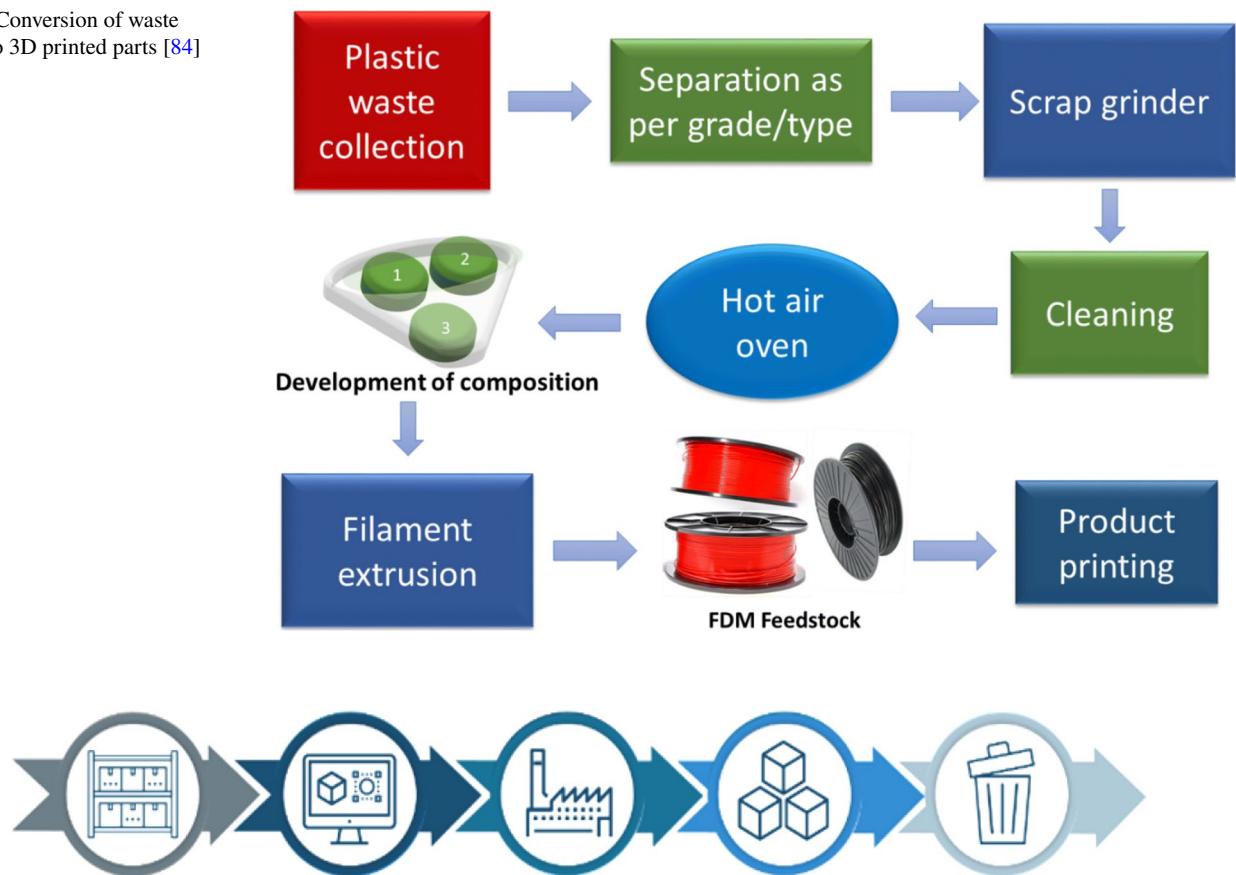


**Fig. 27** The Linear Economy: Raw materials are extracted, transformed into products (often producing waste in the process), and eventually discarded [70]

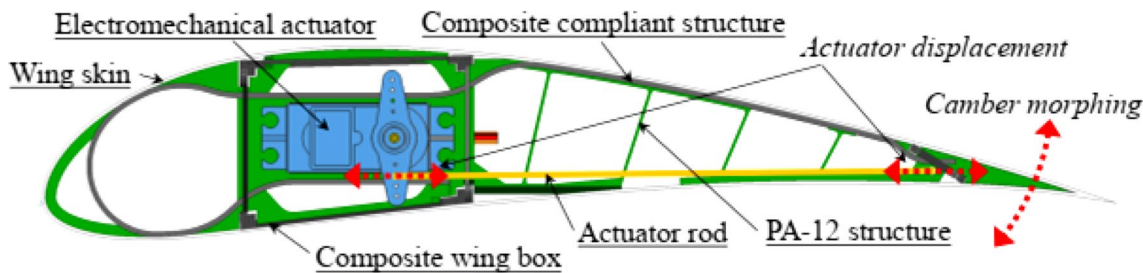


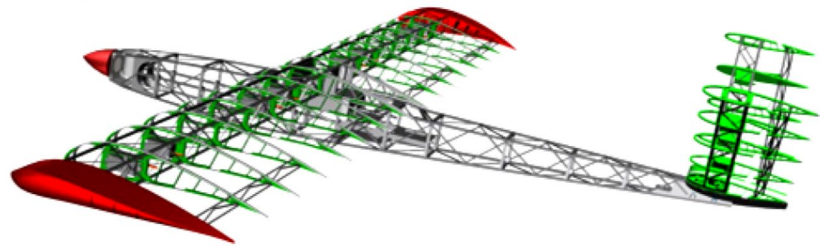
**Fig. 28** Camber morphing concept according to compliant composite structure and electromechanical actuator [103]

- performance). There is a large 4-prong hook with a print weight of nearly 1000 kg involved in this method.
- By combining polymer nanocomposites with continuous fiber reinforcement, strong AM can be achieved resulting in a stronger structure between the layers.
- The combination of experiments and mechanical modeling of fluid and heat flow and in a limited number of additive manufacturing parameters results in the production of printable data efficiently.

- The potential of using recycled polymer in AM has been studied and discussed. The use of recycled materials in the FDM (Fused Deposition Modeling) will contribute to sustainable development and decrease environmental impact. Among AM technologies, FDM is a low-cost technology that employs a thermoplastic filament to build layers of parts.
- There is a high likelihood of composites forming defects in additive manufacturing, reducing their strength. Fiber composites can be developed using the FDM technique,

**Fig. 29** Top: Camber morphing drone concept with Wing box (grey), composite fuselage truss structure, morphing wing-tips (red), and morphing ribs (green). Bottom: Additively manufactured composite drone illustrating morphing actuation [103]

**Drone concept**



**Composite AM drone**



which can decrease the composite processing time and cost.

- The neutron diffraction results obtained from the WAAM in-situ alloyed FeNi in this research have provided a detailed novel viewpoint on the lattice evolution in the FeNi bulk material. WAAM is capable of straightforwardly manufacturing full-density FeNi alloy.
- Aerospace structures can be morphed using composite AM.
- In addition to rapidly manufacturing complex shapes, AM technology can be implemented into medical appli-

cations, provide improved precision and speed, provide product visualization and customization, customized tools, and improve modeling, as well as provide widespread decision-making assistance. AM is introducing a new market to help humanity in the real world.

- Ultrasonic testing UT methods are exceptionally able to identify defects in the engineering components appropriately. Advanced UT techniques like phased array ultrasonic testing (PAUT), guided waves, and laser ultrasonic (LU) have displayed potential in testing AM products. It

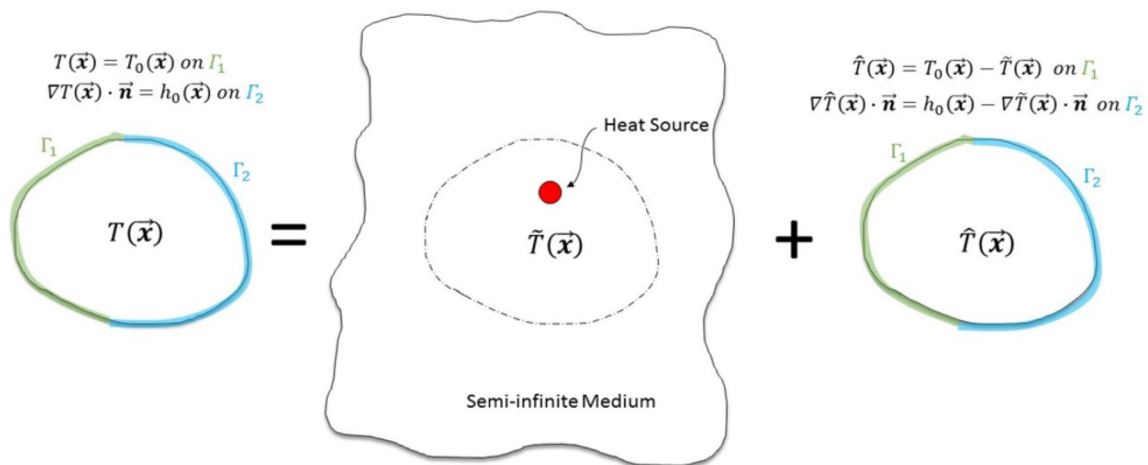


**Fig. 30** representation of the superposition-based finite element method [107]

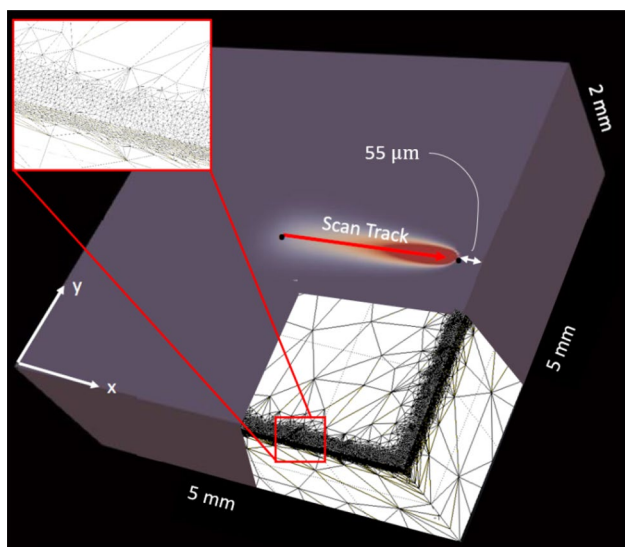


**Fig. 31** 5 mm × 5 mm × 2 mm Single scan model. A graded mesh is superimposed to display the potential computation reduction when comparing the superposition method to traditional FEA [107]

is value studying their capabilities through a comprehensive study.

- AM in the automotive industry is very useful in reproducing and remanufacturing difficult-to-find parts appropriately. As a result, aerospace and automotive engineering, medical sciences, electronics, and related industries

will be the most promising business opportunities for applying to AM soon.

- Process optimization is an efficient method to reduce residual stress and improve bonding between layers in different structures.
- Emissions and gross energy requirements from AM are lesser than machining for buy-to-fly ratios in the life cycle analysis (LCA) work on AM.
- The aerospace industry uses AM due to the feasibility of making lighter structures to decrease weight, which is the general goal of aircraft and spacecraft designers.
- AM technology's most extensively employed steels are stainless steel because of their high strength and suitable ductility.
- AM raises the pitting corrosion resistance of the AM steels generally caused by the quick solidification intrinsic to AM that limits the formation of MnS inclusions.
- Owing to the high printing capacity of PH stainless steel, the 17–4 PH stainless steel is mainly utilized in AM (additive manufacturing).
- Some stainless steels have high strength due to the presence of refined microstructures. These stainless steels include AM 17–4 and 5–15 PH and marl steels 18Ni 300. These steels have less flexible due to additives manufacturing porosity.
- The poor surface finish resulting from the additives manufacturing process leads to poor fatigue resistance in 15–5 and 17–4 PH steels.

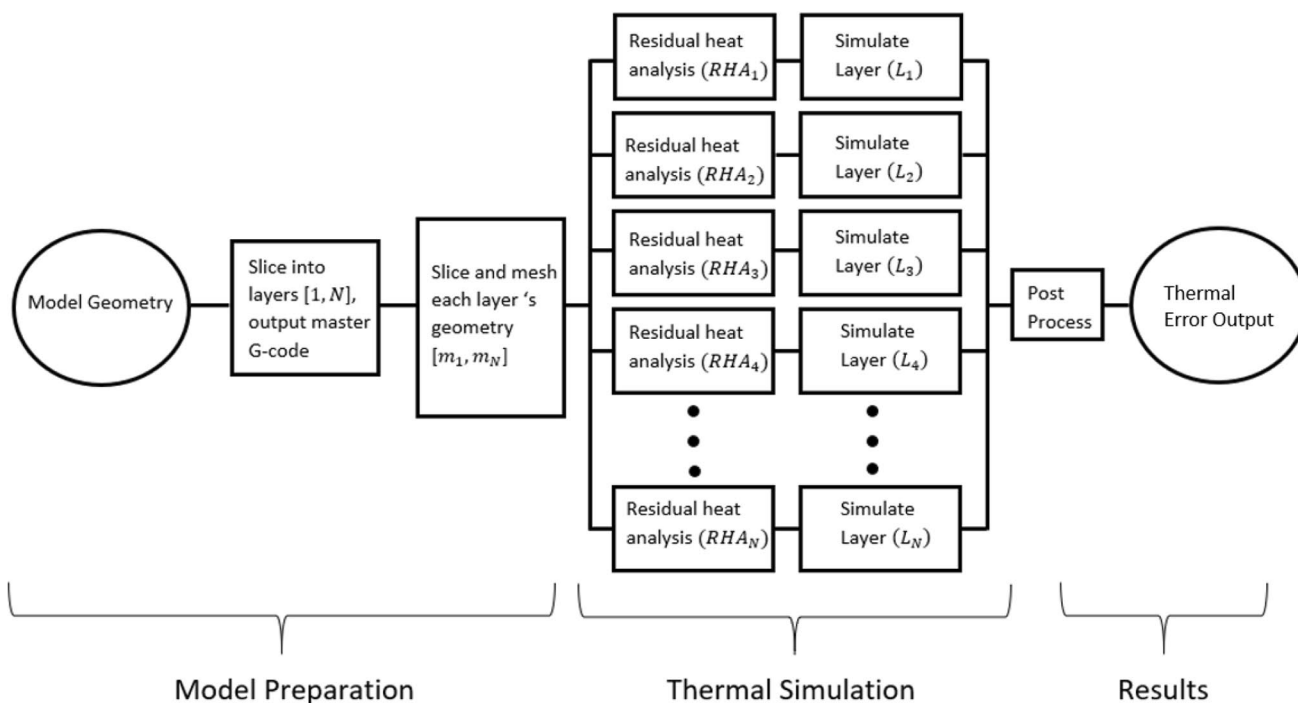


**Fig. 32** Schematic of thermal modeling workflow is divided into model preparation, thermal simulation, and post-processing results [107]

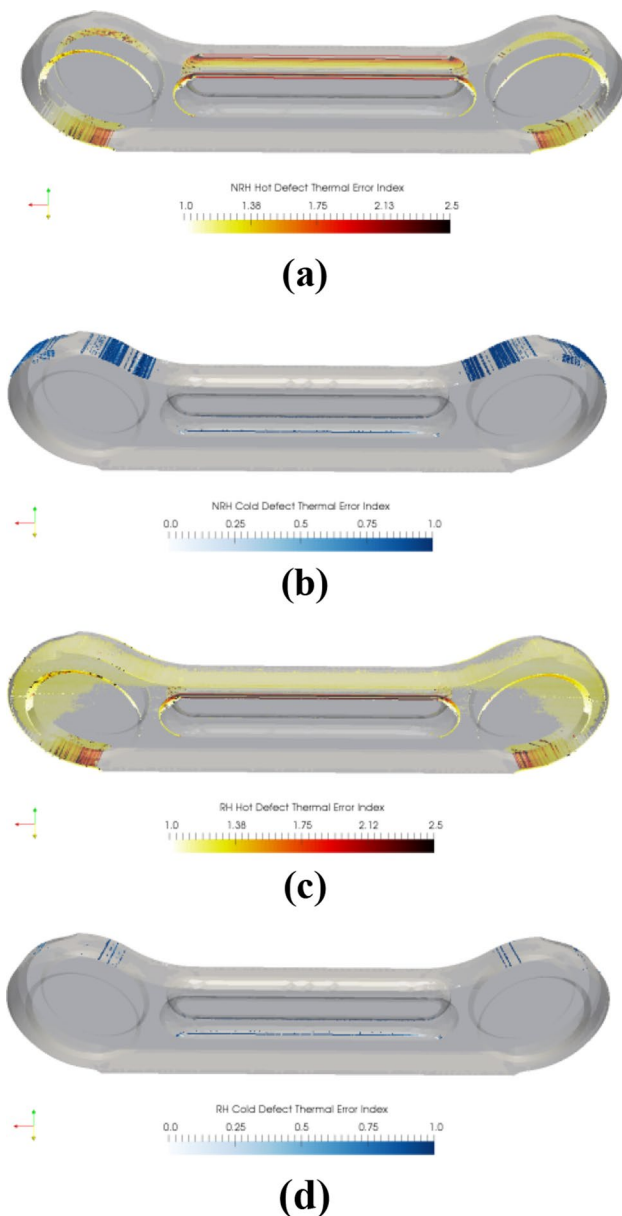


**Fig. 33.** 3D thermal error maps of **a** hot errors with no residual heat **b** cold errors with no residual heat **c** hot errors residual heat **d** cold errors residual heat [107]

- The surface potential of austenite is higher than that of martensite, so AM PHs without solution exhibit greater corrosion resistance.
- As a result of annealing additives in duplex stainless steel, the ultimate tensile strength (UTS) of the steel is reduced, while the length and corrosion resistance of the steel are increased.
- Using additive manufacturing eliminates the need for hardening before austenitizing C-bearing tool steels. The mechanical properties of conventionally processed mate-

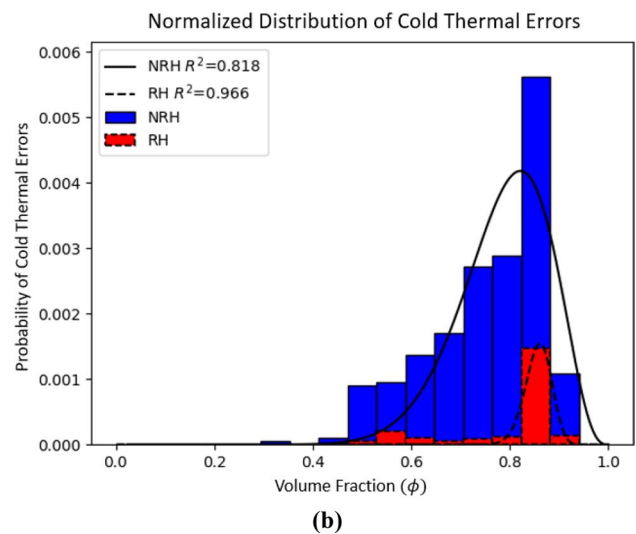
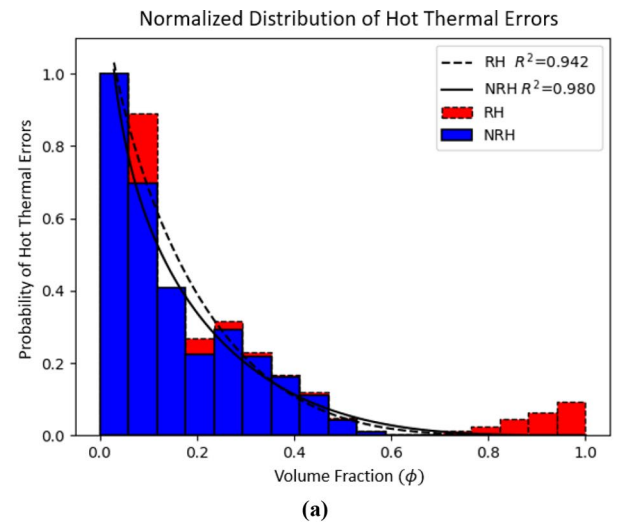


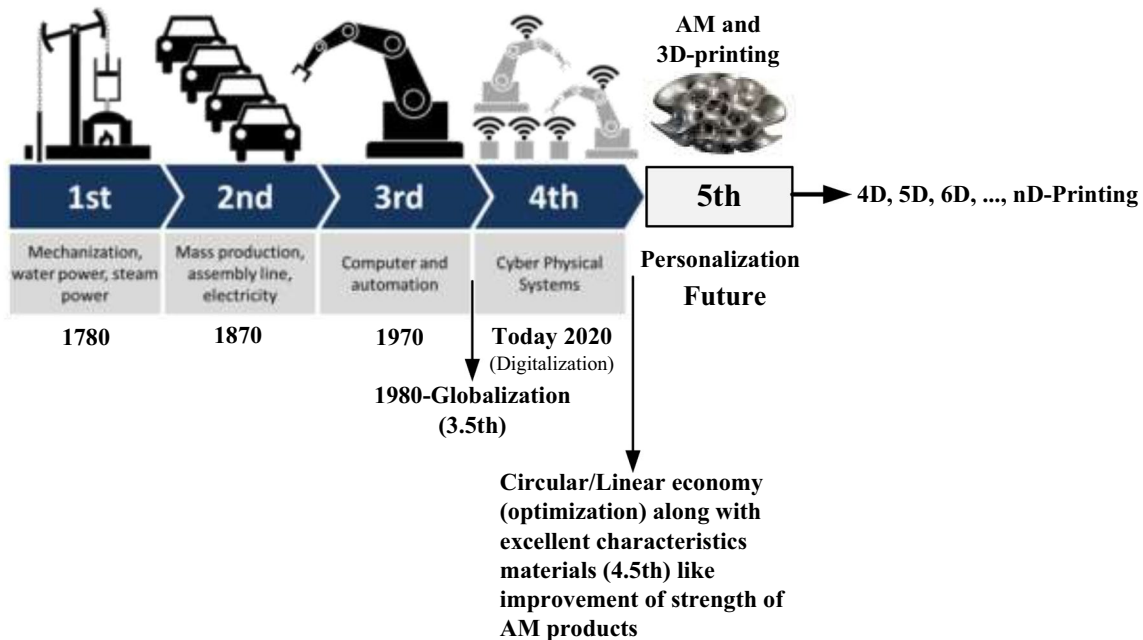
**Fig. 34** The probability distribution for **a** hot and **b** cold thermal errors v. volume fraction for residual heat (RH) and no residual heat (NRH) V-22 link analysis [107]

rials are improved by tempering additive manufacturing components.

- Throughout history, steel has been the most widely used structural engineering material because of its countless design possibilities due to the systematic control of allotropic transformations during thermal treatment. The combination of severe temperature gradients, high cooling rates, and the inherent chemical heterogeneities in AM enables the creation of sole microstructures in steel. Additionally, the exceptional microstructural evolution during AM may necessitate developing new post-processing heat treatment schedules that differ from those developed for usual processing. In addition to residual stresses, microstructural inhomogeneity, poor surface quality, and anisotropy, AM of steels still has a few

**Table 2** Parameters for Beta function least-squared fit of thermal error distributions [107]

Fit parameters				
Simulation	NRH hot errors	NRH cold errors	RH hot errors	Rh cold errors
$\alpha$	0.75	14.9	0.93	147
$\beta$	4.23	4.03	5.31	24.5
$C_o$	0.19	9.46e-04	0.20	1.02e-04
$R^2$	0.980	0.818	0.942	0.966

**Fig. 35** The schematic and modeling of the future towards the fifth industrial revolution/industry 5.0

downsides and limitations. The AM steel parts still have some puzzling attributes, and more research is needed [110].

- Lastly, the schematic and modeling of the future towards the fifth industrial revolution/industry 5.0 are visualized and depicted (proposed/predicted) via a diagram (Fig. 35). In which, AM and nD-printing have excellent development and improvement in the 5<sup>th</sup> industrial revolution.
- Industrial societies have a high request for 4D-printing materials in the aerospace, industrial advanced devices, military, defense, and healthcare industries generally. 4D-printing is an applied result of 3D printing of the smart structures and materials which react and respond to various stimulants to fabricate new practical products. The method and technique of 4D printing have been used in numerous contexts computer engineering sections, and most other engineering fields like mechanical and material engineering, medical devices, and food processing effectively. Recently the study on the topics of 4D-, 5D- and 6D- food printing has been highlighted widely. For

example, 4D-food-printing applications have concentrated and aimed at getting the favorable various colors, shapes, flavors, and nutritional properties of 3D-printed materials. Furthermore, it is noted that 5D- and 6D-printing may in principle print very intricate structures with improved strength and less material than 3D- and 4D-printing.

Moreover, 6D-printing is a novel and different branch of AM studying its benefits, advantages along with probable limitations regarding the design and manufacturing of effective smart materials and structures typically. The mentioned new method combines the 4D- and 5D-printing techniques logically. That is, the printing process is going to employ five degrees of freedom DOF for manufacturing the ultimate item whereas the final manufactured material component would be a smart product. In other words, a 6D-printed structure may be stronger than an equivalent 4D-printed structure, may be fabricated employing less material (low cost), may do movements by being exposed to an external stimulus via an interaction mechanism, and



may learn how to reconfigure itself appropriately, based on predictions through theoretical and mathematical (analytical) modeling and simulations. In the near upcoming, the techniques of 4D-nD printing along with their innovations will be an important section of applied industrial fields, containing the fabrication of high-quality food products which cannot be produced with present processing methods (Fig. 35).

**Data availability** Data sharing does not apply to this article as no datasets were generated or analyzed during the current study.

## Declarations

**Conflict of interest** The authors declare that they have no known competing financial interests or personal relationships that could have appeared to influence the work reported in this paper.

## References

- H. Zhou, H. Yang, S. Yao, L. Jiang, N. Sun, H. Pang, Synthesis of 3D printing materials and their electrochemical applications. *Chin. Chem. Lett.* **33**(8), 3681–3694 (2022). <https://doi.org/10.1016/j.ccllet.2021.11.018>
- A. Zhang, F. Wang, L. Chen, X. Wei, M. Xue, F. Yang, S. Jiang, 3D printing hydrogels for actuators: a review. *Chin. Chem. Lett.* **32**(10), 2923–2932 (2021). <https://doi.org/10.1016/j.ccllet.2021.03.073>
- J. Yang, Y. Cheng, X. Gong, S. Yi, C.-W. Li, L. Jiang, C. Yi, An integrative review on the applications of 3D printing in the field of in vitro diagnostics. *Chin. Chem. Lett.* **33**(5), 2231–2242 (2022). <https://doi.org/10.1016/j.ccllet.2021.08.105>
- S.B. Khan, S. Irfan, S.S. Lam, X. Sun, S. Chen, 3D printed nanofiltration membrane technology for waste water distillation. *J. Water Process Eng.* **49**, 102958 (2022). <https://doi.org/10.1016/j.jwpe.2022.102958>
- M. Karimi, A. Asefnejad, D. Aflaki, A. Surendar, H. Baharifar, S. Saber-Samandari, A. Khandan, A. Khan, D. Toghraie, Fabrication of shapeless scaffolds reinforced with baghdadite-magnetite nanoparticles using a 3D printer and freeze-drying technique. *J. Mater. Res. Technol.* **14**, 3070–3079 (2021). <https://doi.org/10.1016/j.jmrt.2021.08.084>
- X. Du, M. Dehghani, N. Alsaadi, M.G. Nejad, S. Saber-Samandari, D. Toghraie, C.-H. Su, H.C. Nguyen, A femoral shape porous scaffold bio-nanocomposite fabricated using 3D printing and freeze-drying technique for orthopedic application. *Mater. Chem. Phys.* **275**, 125302 (2022). <https://doi.org/10.1016/j.matchemphys.2021.125302>
- A. Moarrefzadeh, M.R. Morovvati, S.N. Angili, G.F. Smaism, A. Khandan, D. Toghraie, Fabrication and finite element simulation of 3D printed poly L-lactic acid scaffolds coated with alginate/carbon nanotubes for bone engineering applications. *Int. J. Biol. Macromol.* **224**, 1496–1508 (2023). <https://doi.org/10.1016/j.ijbiomac.2022.10.238>
- X. Niu, S. Zhu, J. He, D. Liao, J.A.F.O. Correia, F. Berto, Q. Wang, Defect tolerant fatigue assessment of AM materials: size effect and probabilistic prospects. *Int. J. Fatigue* **160**, 106884 (2022). <https://doi.org/10.1016/j.ijfatigue.2022.106884>
- J. He, S. Zhu, C. Luo, X. Niu, Q. Wang, Size effect in fatigue modelling of defective materials: application of the calibrated weakest-link theory. *Int. J. Fatigue* **165**, 107213 (2022). <https://doi.org/10.1016/j.ijfatigue.2022.107213>
- D. Liao, S. Zhu, B. Keshtegar, G. Qian, Q. Wang, Probabilistic framework for fatigue life assessment of notched components under size effects. *Int. J. Mech. Sci.* **181**, 105685 (2020). <https://doi.org/10.1016/j.ijmecsci.2020.105685>
- W. Ren, J. Mazumder, In-situ porosity recognition for laser additive manufacturing of 7075-Al alloy using plasma emission spectroscopy. *Sci. Rep.* **10**, 19493 (2020). <https://doi.org/10.1038/s41598-020-75131-4>
- J. Greer, Julia Greer answers questions about additive manufacturing. *Nat. Commun.* **11**, 3993 (2020). <https://doi.org/10.1038/s41467-020-17723-2>
- A. Boydston, Andrew Boydston answers questions about additive manufacturing. *Nat. Commun.* **11**, 3992 (2020). <https://doi.org/10.1038/s41467-020-17722-3>
- P. Lee, Peter Lee answers questions about additive manufacturing. *Nat. Commun.* **11**, 3995 (2020). <https://doi.org/10.1038/s41467-020-17732-1>
- R. Langer, M. Tibbitt, Answer questions about additive manufacturing. *Nat. Commun.* **11**, 3994 (2020). <https://doi.org/10.1038/s41467-020-17724-1>
- M.A. Ghanem, A. Basu, R. Behrou, N. Boechler, A.J. Boydston, S.L. Craig, Y. Lin, B.E. Lynde, A. Nelson, H. Shen, D.W. Storti, The role of polymer mechanochemistry in responsive materials and additive manufacturing. *Nat. Rev. Mater.* **6**, 84–98 (2021). <https://doi.org/10.1038/s41578-020-00249-w>
- T. DebRoy, T. Mukherjee, H.L. Wei, J.W. Elmer, J.O. Milewski, Metallurgy mechanistic models and machine learning in metal printing. *Nat. Rev. Mater.* **6**, 48–68 (2021). <https://doi.org/10.1038/s41578-020-00236-1>
- T.G. Aguirre, L. Fuller, A. Ingrole, T.W. Seek, B.B. Wheatley, B.D. Steineman, T.L. Haut Donahue, S.W. Donahue, Bioinspired material architectures from bighorn sheep horncore velar bone for impact loading applications. *Sci. Rep.* **10**, 18916 (2020). <https://doi.org/10.1038/s41598-020-76021-5>
- E. Skliutas, M. Lebedevaite, S. Kasetaitė, S. Reškštytė, S. Lileikis, J. Ostrauskaite, M. Malinauskas, A Bio-Based Resin for a Multi-Scale Optical 3D Printing. *Sci. Rep.* **10**, 758 (2020). <https://doi.org/10.1038/s41598-020-66618-1>
- J. Knoška, L. Adriano, S. Awel, K.R. Beyerlein, O. Yefanov, D. Oberthuer, G.E. Peña Murillo, N. Roth, I. Sarrou, P. Villanueva-Perez, M.O. Wiedorn, F. Wilde, S. Bajt, H.N. Chapman, M. Heymann, Ultracompact 3D microfluidics for time-resolved structural biology. *Nat. Commun.* **11**, 657 (2020). <https://doi.org/10.1038/s41467-020-14434-6>
- P.K. Arora, R. Arora, A. Haleemc, H. Kumar, Application of additive manufacturing in challenges posed by COVID-19. *Mater. Today* **38**, 466–468 (2021). <https://doi.org/10.1016/j.matpr.2020.08.323>
- D. Puppi, F. Chiellini, Biodegradable polymers for biomedical additive manufacturing. *Appl. Mater. Today* **20**, 100700 (2020). <https://doi.org/10.1016/j.apmt.2020.100700>
- M. Seyyedi, A. Molajou, Nanohydroxyapatite loaded-acrylated polyurethane nanofibrous scaffolds for controlled release of paclitaxel anticancer drug. *J. Res. Sci. Eng. Technol.* **9**(1), 50–61 (2021).
- S.S. Shetty, M. Sharma, S.P. Kabekkodu, N.V. Anil Kumar, K. Satyamoorthy, R. Radhakrishnan, Understanding the molecular mechanism associated with reversal of oral submucous fibrosis targeting hydroxyllysine aldehyde-derived collagen cross-links. *J. Carcinog.* **20**, 9 (2021). [https://doi.org/10.4103/jcar.JCar\\_24\\_20](https://doi.org/10.4103/jcar.JCar_24_20)
- E.R. Ghomi, F. Khosravi, R.E. Neisiany, S. Singh, S. Ramakrishna, Future of additive manufacturing in healthcare. *Current*

- Opinion Biomed. Eng. **17**, 100255 (2021). <https://doi.org/10.1016/j.cobme.2020.100255>
26. C. Prakash, S. Singh, S. Ramakrishna, Characterization of indigenously coated biodegradable magnesium alloy primed through novel additive manufacturing assisted investment casting. *Mater. Lett.* **275**, 128137 (2020). <https://doi.org/10.1016/j.matlet.2020.128137>
  27. N. Ranjan, R. Singh, I.P.S. Ahuja, M. Rahman, S. Ramakrishna, PLA-HAp-CS-based biocompatible scaffolds prepared through micro-additive manufacturing: a review and future applications, in *3D Printing in Biomedical Engineering*, ed. by S. Singh, C. Prakash, R. Singh (Springer, Singapore, 2020). pp. 209–229. [https://doi.org/10.1007/978-981-15-5424-7\\_10](https://doi.org/10.1007/978-981-15-5424-7_10)
  28. S.P. Murray, K.M. Pusch, A.T. Polonsky, C.J. Torbet, G.G.E. Seward, N. Zhou, S.A.J. Forsik, P. Nandwana, M.M. Kirka, R.R. Dehoff, W.E. Slye, T.M. Pollock, A defect-resistant Co–Ni superalloy for 3D printing. *Nat. Commun.* **11**, 4975 (2020). <https://doi.org/10.1038/s41467-020-18775-0>
  29. P. Kürsteiner, M.B. Wilms, A. Weisheit, B. Gault, E.A. Jägler, D. Raabe, High-strength damascus steel by additive manufacturing. *Nature* **582**, 515–519 (2020). <https://doi.org/10.1038/s41586-020-2409-3>
  30. S. Zhao, G. Siqueira, S. Drdova, D. Norris, C. Ubert, A. Bonnin, S. Galmardini, M. Ganobjak, Z. Pan, S. Brunner, G. Nyström, J. Wang, M.M. Koebel, W.J. Malfait, Additive manufacturing of silica aerogels. *Nature* **584**, 387–392 (2020). <https://doi.org/10.1038/s41586-020-2594-0>
  31. Z. Zhu, D.W.H. Ng, H.S. Park, M.C. McAlpine, 3D-printed multi-functional materials enabled by artificial-intelligence-assisted fabrication technologies. *Nat. Rev. Mater.* **6**, 27–47 (2021). <https://doi.org/10.1038/s41578-020-00235-2>
  32. X. Chen, C. Qiu, In-situ development of a sandwich microstructure with enhanced ductility by laser reheating of a laser melted titanium alloy. *Sci. Rep.* **10**, 15870 (2020). <https://doi.org/10.1038/s41598-020-72627-x>
  33. D. Loterie, P. Delrot, C. Moser, High-resolution tomographic volumetric additive manufacturing. *Nat. Commun.* **11**, 852 (2020). <https://doi.org/10.1038/s41467-020-14630-4>
  34. T.J. Wallin, L.-E. Simonsen, W. Pan, K. Wang, E. Giannelis, R.F. Shepherd, Y. Mengüç, 3D printable tough silicone double networks. *Nat. Commun.* **11**, 4000 (2020). <https://doi.org/10.1038/s41467-020-17816-y>
  35. I. Liaschenko, J. Rosell-Llompart, A. Cabot, Ultrafast 3D printing with submicrometer features using electrostatic jet deflection. *Nature Commun.* **11**, 753 (2020). <https://doi.org/10.1038/s41467-020-14557-w>
  36. D. Jia, F. Li, Y. Zhang, 3D-printing process design of lattice compressor impeller based on residual stress and deformation. *Sci. Rep.* **10**, 600 (2020). <https://doi.org/10.1038/s41598-019-57131-1>
  37. A. Förner, S. Giese, C. Arnold, P. Felfer, C. Körner, S. Neumeier, M. Göken, Nanoscaled eutectic NiAl-(Cr, Mo) composites with exceptional mechanical properties processed by electron beam melting. *Sci. Rep.* **10**, 15153 (2020). <https://doi.org/10.1038/s41598-020-72093-5>
  38. A.K. Srivastava, N. Kumar, A.R. Dixit, Friction stir additive manufacturing—an innovative tool to enhance mechanical and microstructural properties. *Mater. Sci. Eng. B* **263**, 114832 (2021). <https://doi.org/10.1016/j.mseb.2020.114832>
  39. A. Mukhopadhyay, P. Sana, Mechanical and microstructural characterization of Aluminium powder deposit made by friction stir based additive manufacturing. *J. Mater. Process. Technol.* **281**, 116648 (2020). <https://doi.org/10.1016/j.jmatprotec.2020.116648>
  40. Y. Li, C. He, J. Wei, Z. Zhang, G. Qin, X. Zhao, Correlation of local microstructures and mechanical properties of Al–Zn–Mg–Cu alloy build fabricated via underwater friction stir additive manufacturing. *Mater. Sci. Eng. A* **805**, 140590 (2021). <https://doi.org/10.1016/j.msea.2020.140590>
  41. C. He, Y. Li, Z. Zhang, J. Wei, X. Zhao, Investigation on microstructural evolution and property variation along building direction in friction stir additive manufactured Al–Zn–Mg alloy. *Mater. Sci. Eng. A* **777**, 139035 (2020). <https://doi.org/10.1016/j.msea.2020.139035>
  42. G. Moeini, S.V. Sajadifar, T. Engler, B. Heider, T. Niendorf, M. Oechsner, S. Bohm, Effect of friction stir processing on microstructural, mechanical, and corrosion properties of Al–Si12 additive manufactured components. *Metals* **10**, 85 (2020). <https://doi.org/10.3390/met10010085>
  43. P.R. Rajasekaran, A.A. Chapin, D.N. Quan, J. Herberholz, W.E. Bentley, R. Ghodssi, 3D-Printed electrochemical sensor-integrated transwell systems. *Microsyst. Nanoeng.* **6**, 100 (2020). <https://doi.org/10.1038/s41378-020-00208-z>
  44. T. Kunimine, R. Miyazaki, Y. Yamashita, Y. Funada, Effects of laser-beam defocus on microstructural features of compositionally graded WC/Co-alloy composites additively manufactured by multi-beam laser directed energy deposition. *Sci. Rep.* **10**, 8975 (2020). <https://doi.org/10.1038/s41598-020-65429-8>
  45. V. Thampy, A.Y. Fong, N.P. Calta, J. Wang, A.A. Martin, P.J. Depond, A.M. Kiss, G. Guss, Q. Xing, R.T. Ott, A. van Buuren, M.F. Toney, J.N. Weker, M.J. Kramer, M.J. Matthews, C.J. Tassone, K.H. Stone, Subsurface cooling rates and microstructural response during laser based metal additive manufacturing. *Sci. Rep.* **10**, 1981 (2020). <https://doi.org/10.1038/s41598-020-58598-z>
  46. W. Woo, J.S. Jeong, D.K. Kim, C.M. Lee, S.H. Choi, J.Y. Suh, S.Y. Lee, S. Harjo, T. Kawasaki, Stacking fault energy analyses of additively manufactured stainless steel 316L and CrCoNi medium entropy alloy using in situ neutron diffraction. *Sci. Rep.* **10**, 1350 (2020). <https://doi.org/10.1038/s41598-020-58273-3>
  47. C.J. Todaro, M.A. Easton, D. Qiu, D. Zhang, M.J. Birmingham, E.W. Lui, M. Brandt, D.H. StJohn, M. Qian, Grain structure control during metal 3D printing by high-intensity ultrasound. *Nat. Commun.* **11**, 142 (2020). <https://doi.org/10.1038/s41467-019-13874-z>
  48. C.C. Cook, E.J. Fong, J.J. Schwartz, D.H. Porcincula, A.C. Kaczmarek, J.S. Oakdale, B.D. Moran, K.M. Champley, C.M. Rackson, A. Muralidharan, R.R. McLeod, M. Shusteff, Highly tunable thiol-ene photoresins for volumetric additive manufacturing. *Adv. Mater.* **32**(47), 2003376 (2020). <https://doi.org/10.1002/adma.202003376>
  49. V. Egorov, U. Gulzar, Y. Zhang, S. Breen, C. O’Dwyer, Evolution of 3D printing methods and materials for electrochemical energy storage. *Adv. Mater.* **32**(29), 2000556 (2020). <https://doi.org/10.1002/adma.202000556>
  50. K. Chen, R. Huang, Y. Li, S. Lin, W. Zhu, N. Tamura, J. Li, Z.W. Shan, E. Ma, RaftingEnabled recovery avoids recrystallization in 3D-printing- repaired single-crystal superalloys. *Adv. Mater.* **2**(12), 1907164 (2020). <https://doi.org/10.1002/adma.201907164>
  51. I. Cooperstein, S.R.K. Chaitanya Indukuri, A. Bouketov, U. Levy, S. Magdassi, 3D printing of micrometer-sized transparent ceramics with on-demand optical-gain properties. *Adv. Mater.* **32**(28), 2001675 (2020). <https://doi.org/10.1002/adma.202001675>
  52. N.A. Traugott, D. Mistry, C. Luo, K. Yu, Q. Ge, C.M. Yakacki, Liquid-crystal-elastomer-based dissipative structures by digital light processing 3D printing. *Adv. Mater.* **32**(28), 2000797 (2020). <https://doi.org/10.1002/adma.202000797>
  53. F. Lai, C. Yang, R. Lian, K. Chu, J. Qin, W. Zong, D. Rao, J. Hofkens, X. Lu, T. Liu, Three-phase boundary in cross-coupled micro-mesoporous networks enabling 3D-printed and ionogel-based quasi-solid-state micro-supercapacitors. *Adv. Mater.*

- 32(40), 2002474 (2020). <https://doi.org/10.1002/adma.202002474>
54. D. Gräfe, S.L. Walden, J. Blinco, M. Wegener, E. Blasco, C. Barner-Kowollik, It's in the fine print: erasable three-dimensional laser-printed micro- and nanostructures. *Angew. Chem.* **59**(16), 6330–6340 (2020). <https://doi.org/10.1002/anie.201910634>
  55. H.A. Houck, P. Müller, M. Wegener, C.B. Kowollik, F.E. Du Prez, E. Blasco, Shining light on poly(ethylene glycol): from polymer modification to 3D laser printing of water erasable microstructures. *Adv. Mater.* **32**(34), 2003060 (2020). <https://doi.org/10.1002/adma.202003060>
  56. R. Kumar, Tertiary and quaternary recycling of thermoplastics by additive manufacturing approach for thermal sustainability. *Mater. Today Proc.* **37**, 2382–2386 (2021). <https://doi.org/10.1016/j.matpr.2020.08.183>
  57. S.A. Jawade, R.S. Joshi, S.B. Desai, Comparative study of mechanical properties of additively manufactured aluminum alloy. *Mater. Today Proc.* **46**, 9270–9274 (2021). <https://doi.org/10.1016/j.matpr.2020.02.096>
  58. P. Kumar, A. Mahamani, B. Durga Prasad, Design and fabrication of screw feeding device in additive manufacturing. *Mater. Today Proc.* **46**, 405–409 (2021). <https://doi.org/10.1016/j.matpr.2020.09.337>
  59. S.R. Singh, P. Khanna, Wire arc additive manufacturing (WAAM): a new process to shape engineering materials. *Mater. Today Proc.* **44**, 118–128 (2021). <https://doi.org/10.1016/j.matpr.2020.08.030>
  60. HUISMAN'S 3D printed WAAM hook, <https://www.werkenbijhuisman.com/innovations/11/3d-printed-crane-hook>
  61. A. Ayed, A. Valencia, G. Bras, H. Bernard, P. Michaud, Y. Balcaen, J. Alexis, Effects of WAAM process parameters on metallurgical and mechanical properties of Ti-6Al-4V deposits, in *Advances in Materials, Mechanics and Manufacturing*, ed. by F. Chaari, M. Barkallah, A. Bouguecha, B. Zouari, M.T. Khabou, M. Kchaou, M. Haddar. 2nd International Conference on Advanced Materials, Mechanics and Manufacturing (A3M'2018), Hammamet, 17–19 December 2018 (Springer, Cham, 2020), pp. 26–35. [https://doi.org/10.1007/978-3-030-24247-3\\_4](https://doi.org/10.1007/978-3-030-24247-3_4)
  62. S. Bagherifard, A. Heydari Astaraee, M. Locati, A. Nawaz, S. Monti, J. Kondás, R. Singh, M. Guagliano, Design and analysis of additive manufactured bimodal structures obtained by cold spray deposition. *Addit. Manuf.* **33**, 101131 (2020). <https://doi.org/10.1016/j.addma.2020.101131>
  63. S. Bagherifard, M. Guagliano, Fatigue performance of cold spray deposits: coating, repair and additive manufacturing case. *Int. J. Fatigue.* **139**, 105744 (2020). <https://doi.org/10.1016/j.ijfatigue.2020.105744>
  64. N. Fan, J. Cizek, C. Huang, X. Xie, Z. Chlup, R. Jenkins, R. Lupoi, S. Yin, A new strategy for strengthening additively manufactured cold spray deposits through in-process densification. *Addit. Manuf.* **36**, 101626 (2020). <https://doi.org/10.1016/j.addma.2020.101626>
  65. C. Chen, Y. Xie, X. Yan, M. Ahmed, R. Lupoi, J. Wang, Z. Ren, H. Liao, S. Yin, Tribological properties of Al/diamond composites produced by cold spray additive manufacturing. *Addit. Manuf.* **36**, 101434 (2020). <https://doi.org/10.1016/j.addma.2020.101434>
  66. W. Wang, P. Han, Y. Wang, T. Zhang, P. Peng, K. Qiao, Z. Wang, Z. Liu, K. Wang, High-performance bulk pure Al prepared through cold spray-friction stir processing composite additive manufacturing. *J. Mater. Res. Technol.* **9**(4), 9073–9079 (2020). <https://doi.org/10.1016/j.jmrt.2020.06.034>
  67. H. Wu, X. Xie, M. Liu, C. Verdy, Y. Zhang, H. Liao, S. Deng, Stable layer-building strategy to enhance cold-spray-based additive manufacturing. *Addit. Manuf.* **35**, 101356 (2020). <https://doi.org/10.1016/j.addma.2020.101356>
  68. R.N. Raelison, M.R. Guéchi, E. Padayodi, In-flight temperature of solid micrometric powders during cold spray additive manufacturing. *Int. J. Thermal Sci.* **157**, 106422 (2020). <https://doi.org/10.1016/j.ijthermalsci.2020.106422>
  69. L.L. Koithara, R.N. Raelison, S. Costil, Flow phenomenon of micron-sized particles during cold spray additive manufacturing: high-speed optic observation and characterization. *Adv. Powder Technol.* **31**(3), 1060–1079 (2020). <https://doi.org/10.1016/j.ap.2019.12.037>
  70. [www.additivemanufacturing.media](http://www.additivemanufacturing.media)
  71. E.J. Parry, J.M. Best, C.E. Banks, Three-dimensional (3D) scanning and additive manufacturing (AM) allows the fabrication of customised crutch grips. *Mater. Today Commun.* **25**, 101225 (2020). <https://doi.org/10.1016/j.mtcomm.2020.101225>
  72. R. Gill, An overview of multi-material along with composite areas generation by changed additive manufacturing. *Mater. Today Proc.* **37**, 3673–3675 (2021). <https://doi.org/10.1016/j.matpr.2020.10.149>
  73. J.P. Oliveira, T.G. Santos, R.M. Miranda, Revisiting fundamental welding concepts to improve additive manufacturing: From theory to practice. *Prog. Mater. Sci.* **107**, 100590 (2020). <https://doi.org/10.1016/j.pmatsci.2019.100590>
  74. V. Chaudhary, S.A. Mantri, R.V. Ramanujan, R. Banerjee, Additive manufacturing of magnetic materials. *Prog. Mater. Sci.* **114**, 100688 (2020). <https://doi.org/10.1016/j.pmatsci.2020.100688>
  75. H. Wu, W.P. Fahy, S. Kim, H. Kim, N. Zhao, L. Pilato, A. Kafi, S. Bateman, J.H. Koo, Recent developments in polymers/polymer nanocomposites for additive manufacturing. *Prog. Mater. Sci.* **111**, 100638 (2020). <https://doi.org/10.1016/j.pmatsci.2020.100638>
  76. N. Sanaei, A. Fatemi, Defects in additive manufactured metals and their effect on fatigue performance: a state-of-the-art review. *Prog. Mater. Sci.* **117**, 100724 (2021). <https://doi.org/10.1016/j.pmatsci.2020.100724>
  77. H.L. Wei, T. Mukherjee, W. Zhang, J.S. Zuback, G.L. Knapp, A. De, T. DebRoy, Mechanistic models for additive manufacturing of metallic components. *Prog. Mater. Sci.* **116**, 100703 (2021). <https://doi.org/10.1016/j.pmatsci.2020.100703>
  78. A. Reichardt, A.A. Shapiro, R. Otis, R.P. Dillon, J.P. Borgogna, B.W. McEnerney, P. Hosemann, A.M. Beesem, Advances in additive manufacturing of metal-based functionally graded materials. *Int. Mater. Rev.* **66**, 1–29 (2021). <https://doi.org/10.1080/09506608.2019.1709354>
  79. J.P. Hughes, P.L. dos Santos, M.P. Down, C.W. Foster, J.A. Bonacin, E.M. Keefe, S.J. Rowley-Neale, C.E. Banks, Single step additive manufacturing (3D printing) of electrocatalytic anodes and cathodes for efficient water splitting. *Sustain. Energy Fuels* **4**, 302–311 (2020). <https://doi.org/10.1039/C9SE00679F>
  80. E. Hosseini, M. Zakertabrizi, A.H. Korayem, Z. Zaker, R. Shahsavari, Orbital overlapping through induction bonding overcomes the intrinsic delamination of 3D-printed cementitious binders. *ACS Nano* **14**(8), 9466–9477 (2020). <https://doi.org/10.1021/acsnano.0c02038>
  81. A. Vyatskikh, R.C. Ng, B. Edwards, R.M. Briggs, J.R. Greer, Additive manufacturing of high-refractive-index, nanoarchitected titanium dioxide for 3D dielectric photonic crystals. *Nano Lett.* **5**, 3513–3520 (2020). <https://doi.org/10.1021/acs.nanolett.0c00454>
  82. H. Canziani, S. Chiera, T. Schuffenhauer, S.P. Kopp, F. Metzger, A. Bück, M. Schmidt, N. Vogel, Bottom up design of composite supraparticles for powder-based additive manufacturing. *Small* **16**(30), 2002076 (2020). <https://doi.org/10.1002/sml.202002076>

83. N.S. Yadavalli, D. Asheghali, A. Tokarev, W. Zhang, J. Xie, S. Minko, Gravity drawing of micro and nanofibers for additive manufacturing of well-organized 3d-nanostructured scaffolds. *Small* **16**(11), 1907422 (2020). <https://doi.org/10.1002/sml.201907422>
84. V. Shanmugam, O. Das, R.E. Neisiany, K. Babu, S. Singh, M.S. Hedenqvist, F. Berto, S. Ramakrishna, Polymer recycling in additive manufacturing: an opportunity for the circular economy. *Mater. Circ. Econ.* **2**, 11 (2020). <https://doi.org/10.1007/s42824-020-00012-0>
85. V. Shanmugam, D.J. Johnson, K. Babu, S. Rajendran, A. Veerasimman, U. Marimuthu, S. Singh, O. Das, R.E. Neisiany, M.S. Hedenqvist, F. Berto, S. Ramakrishna, The mechanical testing and performance analysis of polymer-fibre composites prepared through the additive manufacturing. *Polym. Test.* **93**, 106925 (2021). <https://doi.org/10.1016/j.polymertesting.2020.106925>
86. S. Singh, C. Prakash, S. Ramakrishna, *Additive Manufacturing Foundation Knowledge for the Beginners* (World Scientific, Singapore, 2020). <https://doi.org/10.1142/11953>
87. J.-H. Fu, A.-Y. Lu, N.J. Madden, C.C. Wu, Y.-C. Chen, M.-H. Chiu, K. Hattar, J.A. Krogstad, S.S. Chou, L.-J. Li, J. Kong, V. Tung, Additive manufacturing assisted van der Waals integration of 3D/3D hierarchically functional nanostructures. *Commun. Mater.* **1**, 42 (2020). <https://doi.org/10.1038/s43246-020-0041-2>
88. S.R. Bazaz, O. Rouhi, M.A. Raoufi, F. Ejeian, M. Asadnia, D. Jin, M.E. Warkiani, 3D Printing of inertial microfluidic devices. *Sci. Rep.* **10**, 5929 (2020). <https://doi.org/10.1038/s41598-020-62569-9>
89. A.K. Mazeeva, M.V. Staritsyn, V.V. Bobyr, S.A. Manninen, P.A. Kuznetsov, V.N. Klimov, Magnetic properties of Fe–Ni permalloy produced by selective laser melting. *J. Alloys Compd.* **814**, 152315 (2020). <https://doi.org/10.1016/j.jallcom.2019.152315>
90. B. Li, L. Zhang, W. Fu, H. Xu, General investigations on manufacturing quality of permalloy via selective laser melting for 3d printing of customized magnetic shields. *JOM* **72**, 2834–2844 (2020). <https://doi.org/10.1007/s11837-019-03979-7>
91. V. Chaudhary, N.M.S.K.K. Yadav, S.A. Mantri, A. Jagetia, R.V. Ramanujan, R. Banerjee, Additive manufacturing of functionally graded Co–Fe and Ni–Fe magnetic materials. *J. Alloys Compd.* **823**, 153817 (2020). <https://doi.org/10.1016/j.jallcom.2020.153817>
92. C. Shen, K.-D. Liss, M. Reid, Z. Pan, X. Hua, F. Li, G. Mou, Y. Huang, Y. Zhu, H. Li, Fabrication of FeNi intermetallic using the wire-arc additive manufacturing process: a feasibility and neutron diffraction phase characterization study. *J. Manuf. Process.* **57**, 691–699 (2020). <https://doi.org/10.1016/j.jmapro.2020.07.027>
93. C. Kenel, T. Davenport, X. Li, R.N. Shah, D.C. Dunand, Kinetics of alloy formation and densification in Fe-Ni-Mo microfilaments extruded from oxide- or metal-powder inks. *Acta Mater.* **193**, 51–60 (2020). <https://doi.org/10.1016/j.actamat.2020.04.038>
94. A. Hadadzadeh, B.S. Amirkhiz, S. Shakerin, J. Kelly, J. Li, Mo. Mohammadi, Microstructural investigation and mechanical behavior of a two-material component fabricated through selective laser melting of AlSi10Mg on an Al-Cu-Ni-Fe-Mg cast alloy substrate. *Addit. Manuf.* **31**, 100937 (2020). <https://doi.org/10.1016/j.addma.2019.100937>
95. J.M. Park, J. Choe, H.K. Park, S. Son, J. Jung, T.-S. Kim, J.-H. Yu, J.G. Kim, H.S. Kim, Synergetic strengthening of additively manufactured (CoCrFeMnNi)99C1 high-entropy alloy by heterogeneous anisotropic microstructure. *Addit. Manuf.* **35**, 101333 (2020). <https://doi.org/10.1016/j.addma.2020.101333>
96. H.A. Colorado, E.I. Gutiérrez Velásquez, S.N. Monteiro, Sustainability of additive manufacturing: the circular economy of materials and environmental perspectives. *J. Mater. Res. Technol.* **9**(4), 8221–8234 (2020). <https://doi.org/10.1016/j.jmrt.2020.04.062>
97. F.A. Cruz Sanchez, H. Boudaoud, M. Camargo, J.M. Pearce, Plastic recycling in additive manufacturing: a systematic literature review and opportunities for the circular economy. *J. Cleaner Product.* **264**, 121602 (2020). <https://doi.org/10.1016/j.jclepro.2020.121602>
98. J. Garrido, J. Sáez, J.I. Armesto, A.M. Espada, D. Silva, J. Goikoetxea, A. Arrillaga, B. Lekube, 3D printing as an enabling technology to implement maritime plastic circular economy. *Procedia Manuf.* **51**, 635–641 (2020). <https://doi.org/10.1016/j.promfg.2020.10.089>
99. K. DePalma, M.R. Walluk, A. Murtaugh, J. Hilton, S. Mc Conky, B. Hilton, Assessment of 3D printing using fused deposition modeling and selective laser sintering for a circular economy. *J. Cleaner Product.* **264**, 121567 (2020). <https://doi.org/10.1016/j.jclepro.2020.121567>
100. M. Despeisse, M. Baumers, P. Brown, F. Charnley, S.J. Ford, A. Garmulewicz, S. Knowles, T.H.W. Minshall, L. Mortara, F.P. Reed-Tsochas, J. Rowley, Unlocking value for a circular economy through 3D printing: a research agenda. *Technol. Forecast. Soc. Change* **115**, 75–84 (2017). <https://doi.org/10.1016/j.techfore.2016.09.021>
101. D. Yadav, R.K. Garg, A. Ahlawat, D. Chhabra, 3D printable bio-materials for orthopedic implants: solution for sustainable and circular economy. *Resour. Policy* **68**, 101767 (2020). <https://doi.org/10.1016/j.resourpol.2020.101767>
102. L. Fitzsimons, G. McNamara, M. Obeidi, D. Brabazon, The circular economy: additive manufacturing and impacts for materials processing, in *Encyclopedia of Renewable and Sustainable Materials*, vol. 1, ed. by S. Hashmi, I.A. Choudhury (Elsevier, Amsterdam, 2020), pp. 81–92. <https://doi.org/10.1016/B978-0-12-803581-8.11660-1>
103. U. Fasel, D. Keidel, L. Baumann, G. Cavolina, M. Eichenhofer, P. Ermanni, Composite additive manufacturing of morphing aerospace structures. *Manuf. Lett.* **23**, 85–88 (2020). <https://doi.org/10.1016/j.mfglet.2019.12.004>
104. G. Shi, C. Guan, D. Quan, D. Wu, L. Tang, T. Gao, An aerospace bracket designed by thermo-elastic topology optimization and manufactured by additive manufacturing. *Chin. J. Aeronaut.* **33**(4), 1252–1259 (2020). <https://doi.org/10.1016/j.cja.2019.09.006>
105. M.O. Oyesola, K. Mpofu, N.R. Mathe, I.A. Daniyan, Hybrid-additive manufacturing cost model: a sustainable through-life engineering support for maintenance repair overhaul in the aerospace. *Procedia Manuf.* **49**, 199–205 (2020). <https://doi.org/10.1016/j.promfg.2020.07.019>
106. F. Honarvar, A. Varvani-Farahani, A review of ultrasonic testing applications in additive manufacturing: defect evaluation, material characterization, and process control. *Ultrasonics* **108**, 106227 (2020). <https://doi.org/10.1016/j.ultras.2020.106227>
107. T.P. Moran, D.H. Warner, N. Phan, Scan-by-scan part-scale thermal modelling for defect prediction in metal additive manufacturing additive manufacturing. *Addit. Manuf.* **37**, 101667 (2021). <https://doi.org/10.1016/j.addma.2020.101667>
108. C.-H. Liu, N. Jeyaparakash, C.-H. Yang, Material characterization and defect detection of additively manufactured ceramic teeth using non-destructive techniques. *Ceram. Int.* **47**, 7017–7031 (2021). <https://doi.org/10.1016/j.ceramint.2020.11.052>
109. J. Wilbig, F. Borges de Oliveira, A.-F. Obaton, M. Schwentenwein, K. Rübner, J. Günster, Defect detection in additively manufactured lattices. *Open Ceram.* **3**, 100020 (2020). <https://doi.org/10.1016/j.oceram.2020.100020>
110. N. Haghdadi, M. Laleh, M. Moyle, S. Primig, Additive manufacturing of steels: a review of achievements and challenges.

J. Mater. Sci. **56**, 64–107 (2021). <https://doi.org/10.1007/s10853-020-05109-0>

**Publisher's Note** Springer Nature remains neutral with regard to jurisdictional claims in published maps and institutional affiliations.

Springer Nature or its licensor (e.g. a society or other partner) holds exclusive rights to this article under a publishing agreement with the author(s) or other rightsholder(s); author self-archiving of the accepted manuscript version of this article is solely governed by the terms of such publishing agreement and applicable law.